Reactivation and enrichment of a Gondwana margin Ni-Cu-PGE-(Te-Au) mineral system during the breakup of Pangea

Marco Fiorentini, Steve Denyszyn, Greg Dering
University of Western Australia

David Holwell, Daryl Blanks
University of Leicester, UK

Roland Maas
University of Melbourne, Australia

Marek Locmelis
Missouri University of Science & Technology

Crystal Laflamme
Universite Laval

Abstract. The lower crustal domains of the Ivrea Zone of NW Italy record the polyphase evolution of a Ni-Cu-PGE-(Te-Au) magmatic sulfide mineral system, which formed during multiple stages over an 80 Myr interval along the NW margin of Gondwana. Between 290-250 Ma, a series of hydrated and carbonated ultramafic alkaline pipes containing Ni-Cu-PGE-(Te-Au) mineralisation was emplaced in the lower continental crust of the Ivrea Zone. Subsequently, at 200 Ma Ni-Cu-PGE mineralisation was associated with emplacement of the La Balma-Monte Capio (LBMC) ultramafic intrusion. The composition and metal endowment of the LBMC reflects interaction and mixing between a deeply sourced juvenile and relatively dry primitive magma, most likely associated with the Central Atlantic Magmatic Province, with localised pods enriched in volatiles, metals, sulfur and tellurium, consistent with the composition of the Permo-Triassic pipes. The scenario depicted here may explain why ore deposits along the margins of lithospheric blocks are not distributed homogeneously along their entire extension but generally form clusters. As mineral exploration is essentially a search space reduction exercise, this new understanding may prove to be important in predictive exploration targeting for new mineralised camps, as it provides a way to prioritise segments with enhanced fertility along extensive lithospheric block margins.

1 Introduction

The Ivrea Zone, a well-known section of exhumed lower continental crust in the southern Alps of Italy, was deformed and metamorphosed during the ca. 420–300 Ma Variscan Orogeny, the result of collision between Laurussia and Gondwana during the formation of Pangaea. Following the peak of regional metamorphism, underplating and intrusion of voluminous mafic magmas formed the 287 Ma Mafic Complex (e.g., Peressini et al. 2007; Fiorentini et al. 2018). A series of alkaline pipes containing widespread Ni-Cu-PGE-(Te-Au) mineralisation intruded both the Mafic Complex and the metasedimentary host rocks from 287 Ma to 249 Ma (Fiorentini et al. 2018). Tectonic overprint of the Alpine orogeny from ca. 100 Ma onward was relatively minor and mainly resulted in tilting of the entire section and subsequent exhumation along a major lithospheric boundary marked by the Insubric Line (e.g., Wolff et al. 2012).

Extending north from the Mafic Complex are mafic and ultramafic bodies that have historically been considered as attenuated intrusions emplaced in the lower to middle crust. The largest ultramafic body among these is the La Balma-Monte Capio (LBMC) intrusion, which contains significant Ni-Cu-PGE-(Te-Au) mineralisation. Ferrario et al. (1983) suggested that it formed by *in situ* differentiation of a high-Mg magma emplaced coevally with the Mafic Complex (i.e., at 287 Ma). However, new isotopic and geochronological data presented in Denyszyn et al. (2018) reveal that the LBMC intrusion represents a distinct magmatic event in the Ivrea Zone, with major implications for our understanding of the emplacement of one of the largest large igneous provinces (LIPs) in the geological record, and for the development of a significant mineralisation event.

Mafic and ultramafic magmas that intrude into the lower crust can preserve evidence for transfer of metal and S from the lithospheric mantle into continental crust. The Ni-Cu-PGE-(Te-Au) mineral system archived in the Ivrea Zone illustrates how the lower continental crust can be locally fertilised with mantle-derived metals and volatiles, which are available for later remobilisation into a range of ore systems at various lithospheric depths. It has previously been proposed that the spatial correlation of world-class mineral deposits with the margins of lithospheric blocks is the result of crustal architecture that promotes focused flux of fluids and mantle-derived magmas (Begg et al. 2010). In addition to favourable pathways, our work suggests that localised volatile and metal enrichment of the lower crust related to mantle-derived hydrous (and carbonate) metasomatism plays a role in the distribution of mineral deposits along lithospheric boundaries.

2 The Permo-Triassic Ni-Cu-PGE-(Te-Au) mineral system related to post-collisional gravitational collapse of the Variscan Orogen

Early mineralization is associated with a series of ultramafic, alkaline pipes emplaced after formation of the Mafic Complex, a major crustal underplating event precisely dated via U/Pb CA-IDTIMS on zircon at 286.8 ± 0.4 Ma (Fiorentini et al. 2018). The ultramafic pipes are 100 to 300 m wide and form cumulate-rich conduits that intrude gabbros and dioritic rocks of the Mafic Complex at mid-crustal depths (Demarchi et al. 1998). They are hydrated and carbonated, have unusually high incompatible element concentrations and contain blebby and semi-massive Ni-Cu-PGE sulfide mineralisation.

The sulfides occur as coarse intergranular nodules (> 10 mm) and as small intragranular blebs (< 1 mm) hosted in olivine (Vukmanovic et al. 2018), and have homogeneous, mantle-like $\delta^{34}S$ (Fiorentini et al. 2018). This homogeneity suggests that the pipes reached sulfide supersaturation without addition of crustal sulfur, and that the $\delta^{34}S$ signature is representative of the continental lithospheric mantle. One of the pipes, the 249 Ma Valmaggia pipe, carries a very distinctive Sr- Nd-Hf-Pb isotopic composition, which requires a source with long-term (2500 to 1500 Myr) U-, Th- and Rb-depletion and LREE enrichment (Fiorentini et al. 2018). During post-collisional gravitational collapse of the Variscan Orogen, this source produced the alkaline mafic–ultramafic magma enriched in Ni-Cu-PGE-(Te-Au) and volatiles (H_2O, CO_2, S), which formed the deep-crustal intrusion at Valmaggia. U/Pb dating of other chemically and geologically comparable pipes in the area show that this process was active over at least 40 Myr (Fiorentini et al. 2018).

3 The Jurassic Ni-Cu-PGE mineral system related to emplacement of magmas of the Central Atlantic Magmatic Province

The LBMC intrusion is a north-striking tabular body, approximately 400 m thick and ≥ 3 km long that dips steeply east, concordant with the overlying metasedimentary rocks. Regional tilting effectively exposes a cross section of the intrusion, with basal dunites grading to plagioclase pyroxenites at the top (cf. Ferrario et al. 1983). Magmatic Ni-Cu-PGE mineralization occurs as disseminated, blebby, and locally net-textured sulfides in horizons throughout the intrusion, in places reaching 10% in volume. The roof of the body displays metre-scale intrusive relationships with the overlying high-grade metasedimentary rocks, referred to as the Kinzigite Formation (Garuti et al. 1980). The base of the intrusion is strongly modified by southeast-vergent thrust faults in the footwall of the Insubric Line (Denyszyn et al. 2018). Across this faulted footwall contact, migmatites of the Kinzigite Formation are interlayered with a belt of garnet-bearing gabbros of Permian–Carboniferous age, previously referred to as the Monte Capio sill (Klötzli et al. 2014). The original lateral extent of the LBMC intrusion is unconstrained because of faulting and younger cover.

The LBMC intrusion differs from other mafic-ultramafic bodies in the Ivrea Zone in its geometry and mineralisation style (Garuti et al.1990). It is ~400 m thick and mostly dunitic, compared to the < 30-m-thick pyroxenitic sills in the lowermost Mafic Complex or the Permo-Triassic < 300-m-wide alkaline pipes emplaced within the Mafic Complex and Kinzigite Formation.

The recent precise U/Pb CA-IDTIMS age of 200 Ma led Denyszyn et al. (2018) to suggest the LBMC intrusion is a deep and distal expression of the Central Atlantic Magmatic Province (CAMP), which is related to the opening of the central Atlantic Ocean and thus the breakup of Pangaea (e.g., Ruiz-Martínez et al. 2012). The driver for CAMP magmatism may be a mantle plume (e.g., Wilson 1997), though thermal anomalies inducing mantle melting in the absence of any deeper mantle source have also been proposed (e.g., McHone 2000). New information from trace element geochemistry as well as stable and radiogenic isotopes indicates that the composition of the LBMC intrusion reflects interaction and mixing between a deeply sourced juvenile and relatively dry primitive magma, most likely associated with the CAMP (Denyszyn et al. 2018), with localised pods enriched in volatiles, metals, S and Te, consistent with the composition of the Permo-Triassic pipes (Fiorentini et al. 2018).

The results presented in this study, which include new field observations integrated with petrological, geochemical and isotopic data, constrain the internal architecture of the LBMC intrusion and question the existing interpretation of formation as a layered sequence produced by in situ fractionation (Ferrario et al. 1983). New mapping and structural analyses combined with thermodynamic modelling of this largely dunitic body have implications for emplacement dynamics and the geodynamic setting of intrusion and mineralisation. The outcome of our work supports the hypothesis of Fiorentini et al. (2018) that enhanced potential for ore formation at lithospheric margins may be due not only to favourable architecture conducive to focussing of magmas and fluids (e.g., Begg et al. 2010; Mole et al. 2013), but also to localised enhanced metal and volatile fertility (cf. Laflamme et al. 2018).

4 The lower crust as a key to fertility

At the time of emplacement of the LBMC intrusion, the physical and chemical structure of the crust in the Ivrea Zone had been strongly modified by emplacement of the Mafic Complex > 80 Ma earlier. The process of magmatic underplating in the Ivrea Zone (e.g., Quick et al. 2009) has been compared to layering and densification of lower continental crust in other extensional terranes, such as the central Basin and Range province (western North America; Rutter et al. 1993), yet the long-term effects of these physical changes on crustal evolution and the effects on later magmatic episodes are poorly known.

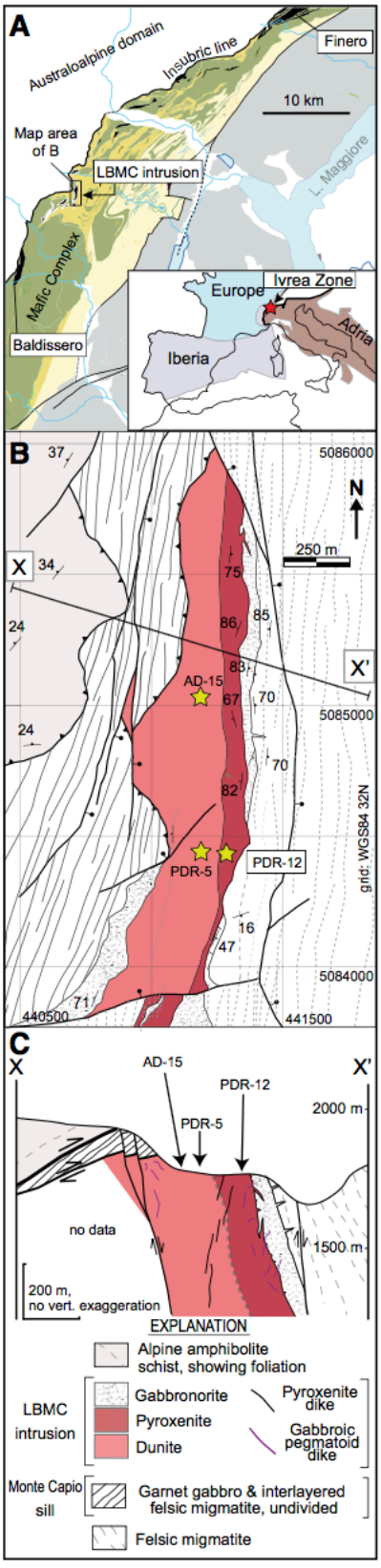

Figure 1. Regional geological map showing location of La Balma–Monte Capio (LBMC) intrusion, southern Alps, Italy. Finero and Baldissero are mantle tectonites outcropping in the area. B: Local geological map of LBMC intrusion, with locations (stars) of samples dated in Denyszyn et al. (2018). Coordinates given in UTM system, zone 32N. C: Cross section through LBMC intrusion.

As Denyszyn et al. (2018) discussed, the LBMC intrusion seems to have exploited the transition in the lower crust where the Permian underplate (i.e., the Mafic Complex) is in contact with metasedimentary host rocks (i.e., the Kinzigite Formation). Studies of the structural position of the LBMC intrusion with respect to such petrological and rheological boundaries may yield insight into mechanisms of magma ascent and arrest in the lower crust.

The proposed temporal and genetic link between 200 Ma magmatism in the Ivrea Zone and the CAMP is supported by the position of the Ivrea Zone near a major lithospheric suture, the Insubric Line, which separates the European and Adria plates. Emplacement of mantle-derived magmas is commonly localised along lithospheric boundaries (Gorczyk et al. 2017), as is the occurrence of magmatic Ni-Cu-PGE mineralisation (Begg et al. 2010), preferentially in areas where previous S and metal enrichment of the lower continental crust may enhance localised sulfide saturation in ascending mantle-derived magmas (Fiorentini et al. 2018). The crustal suture represented by the Insubric Line may have created pathways that promoted interaction of CAMP-related magma with pre-existing metal- and volatile-enriched pipes stored in the lower crust.

The scenario depicted here may explain why ore deposits along the margins of lithospheric blocks are not distributed homogeneously along their entire extension but generally form clusters. As mineral exploration is essentially a search space reduction exercise, this new understanding may prove to be important in predictive exploration targeting for new mineralised camps, as it provides a way to prioritise segments with enhanced fertility along extensive lithospheric block margins.

Acknowledgements

This work is funded by the Australian Research Council grant" Metal Sources and Transport Mechanisms in the Deep Lithosphere" Centre of Excellence for Core to Crust Fluid Systems (CCFS, CE11E0070) and by NERC grant NE/M010848/1 "TeaSe: tellurium and selenium cycling and supply" awarded to the University of Leicester.

References

Peressini G, Quick JE, Sinigoi S, Hofmann AW, Fanning M (2007) Duration of a Large Mafic Intrusion and Heat Transfer in the Lower Crust: a SHRIMP U/Pb Zircon Study in the Ivrea-Verbano Zone (Western Alps, Italy). J Pet 48:1185-1218.

Begg GC, Hronsky JA, Arndt NT, Griffin WL, O'Reilly SY, Hayward N (2010) Lithospheric, cratonic, and geodynamic setting of Ni-Cu-PGE sulfide deposits. Economic geology, 105(6):1057-1070.

Demarchi G, Quick JE, Sinigoi S, Mayer A (1998) Pressure gradient and original orientation of a lower-crustal intrusion in the Ivrea-Verbano Zone, Northern Italy. Journal of Geology 106:609-622. 10.1086/516045.

Denyszyn SW, Fiorentini ML, Maas R, Dering G (1998) A bigger tent for CAMP. Geology 46 (9):823-826

Ferrario A, Garuti G, Rossi A, Sighinoi GP (1983) Petrographic and metallogenic outlines of the "La Balma–M. Capio" ultrama c-ma c body (Ivrea-Verbano basic complex, NW Italian Alps), in

Schneider, H.J., ed., Mineral Deposits of the Alps and of the Alpine Epoch in Europe: Berlin Heidelberg, Springer-Verlag, 28–40, https://doi .org/10.1007/978-3-642-68988-8_4.
Fiorentini ML, LaFlamme C, Denyszyn S, Mole D, Maas R, Locmelis M, Caruso S, Bui T-H (2018) Post-collisional alkaline magmatism as gateway for metal and sulfur enrichment of the lower crust: Geochimica et Cosmochimica Acta, 223:175–197, https://doi.org/10.1016 /j.gca.2017.11.009.
Garuti G, Rivalenti G, Rossi A, Siena F, Sinigoi S (1980) The Ivrea-Verbano ma c ultrama c complex of the Italian western Alps: Discussion of some petrologic problems and a summary: Rendiconti della Società Italiana di Mineralogia e Petrologia, 36:717–749.
Garuti G, Naldrett AJ, Ferrario A (1990) Platinum-group elements in magmatic sul des from the Ivrea Zone: Their control by sul de assimila- tion and silicate fractionation: Economic Geol- ogy and the Bulletin of the Society of Economic Geologists, 85:328–336, https://doi.org/10.2113/gsecongeo.85.2.328.
Gorczyk W, Mole DR, Barnes SJ (2017) Plume-lithosphere interaction at craton margins throughout Earth history: Tectonophysics, 746:678-694, https:// doi.org/10.1016/j.tecto.2017.04.002.
Klötzli US, Sinigoi S, Quick JE, Demarchi G, Tassinari CCG, Sato K, Günes Z (2014) Duration of igneous activity in the Sesia Mag- matic System and implications for high-temper- ature metamorphism in the Ivrea-Verbano deep crust: Lithos, 206–207:19–33, https://doi.org/10.1016/j.lithos.2014.07.020.
Laflamme C, Fiorentini M, Lindsay M, Bui T (2018) Atmospheric sulfur is recycled to the crystalline continental crust during supercontinent formation. Nature Communications 9.
McHone JG (2000) Non-plume magmatism and rifting during the opening of the central Atlantic Ocean: Tectonophysics, v. 316, p. 287–296, https://doi.org/10.1016/S0040-1951(99)00260-7.
Mole DR, Fiorentini ML, Cassidy KF, Kirkland CL, Thebaud N, McCuaig TC, Doublier MP, Duuring P, Romano SS, Maas R, Belousova EA, Barnes SJ, Miller J (2013) Crustal evolution, intra-cratonic architecture and the metallogeny of an Archaean craton, Geological Society, London, Special Publications, 393:23-80.
Quick JE, Sinigoi S, Peressini G, Demarchi G, Wooden JL, Sbisà A (2009) Magmatic plumbing of a large Permian caldera exposed to a depth of 25 km: Geology, 37:603–606, https://doi.org/10.1130/G30003A.1.
Ruiz-Martínez VC, Torsvik TH, van Hinsbergen DJJ, Gaina C (2012) Earth at 200 Ma: Global palaeogeography re ned from CAMP pa- laeomagnetic data: Earth and Planetary Science Letters, 331–332:67–79, https://doi.org/10.1016/j.epsl.2012.03.008.
Rutter EH, Brodie KH, Evans PJ (1993) Structural geometry, lower crustal magmatic un- derplating and lithospheric stretching in the Ivrea- Verbano zone, northern Italy: Journal of Struc- tural Geology, 15:647–662, https://doi.org /10.1016/0191-8141(93)90153-2.
Vukmanovic Z, Fiorentin ML, Reddy SM, Godel B (2018) Microstructural constraints on magma emplacement and sulfide transport mechanisms, Lithosphere, 11, 73-90.
Wilson M. (1997) Thermal evolution of the Central Atlantic passive margins: Continental break-up above a Mesozoic super-plume: Journal of the Geological Society, 154:491–495, https://doi.org/10.1144/gsjgs.154.3.0491.
Wolff R, Dunkl I, Kiesselbach G, Wemmer K, Siegesmund S, 2012, Thermochronological constraints on the multiphase exhumation history of the Ivrea-Verbano Zone of the Southern Alps: Tectonophysics, 579:104–117, https://doi.org/10.1016/j.tecto.2012.03.019.

Formation and disruption of Cu-Ni-PGE deposits in a giant deep-seated mafic-ultramafic conduit system

Rune B. Larsen, Bjørn E. Sørensen, Even Nikolaisen
Department of Geosciences and Petroleum, NTNU, Trondheim, Norway

Abstract. The Central Iapetus Magmatic Province (CIMP, Ma 610-560) is a prominent worldwide LIP, well known from Greenland, Labrador, North America, the Baltic shield and South Africa. The Seiland Igneous Province (SIP) forming at Ma 570-520, in NW-Norway comprises the most deep-seated parts of the CIMP event (0.6-1.0 GPa). The SIP is a high yielding, mafic-ultramafic-alkaline conduit system conveying thousands of km^3 of melts from the asthenosphere to the continental lithosphere. In the SIP, we have located several meter's wide sub-horisontal Cu-Ni-PGE occurrences in the Reinfjord ultramafic conduit system (Fig. 1). The deposits carry up to 1.7 g/t total PGE with c. 75% PPGE+Au and 25 % IPGE including 0.2 g/t osmium. Other deposits have c. 0.1 wt% Cu and up to 0.4 wt% Ni i.e. they are not particularly rich, however, with thicknesses of 10-20 meters over >0.5 Km^2, they represent considerable tonnages. The PGE and Cu+Ni occurrences are decoupled. The PGE-horizons are mostly situated in dunitic cumulates, which formed from picritic melts in the most primitive parts of the intrusion. The sulphides as well as the PGMs are closely associated with carbonated as well as hydrous mineral assemblages that formed from immiscible alkaline melts that are co-genetic with and/or dissolved in the picritic melts and may play an important role in both formation and remobilization of the immiscible sulphide droplets.

1 Significance of large deep-seated conduit system

The upper crustal expressions of large magmatic events are documented in several well-exposed Large Igneous Provinces (LIP's) (e.g., Ernst and Bell, 2010). Problematically, the shallow intrusive and extrusive products of LIP magmatism represent a system that has lost many of its key components during ascent through 30-50 km of crust and during surface eruptions. Not least when melts and volatile-rich phases pass through and become altered in intermittent magma-chambers en route to the shallow crust or the surface. Therefore, lavas and shallow sills provide a biased and distant record of the primary magmas and deep crustal processes that likely govern composition, tempo, and outgassing (e.g., Cox et al. 1980). Equally important, the transfer of economic metals such as Cu, Ni and the PGE's from the mantle to the lower crust is poorly constrained.

This is a very serious gap in our knowledge because the primary chemical as well as physical properties of lower lithospheric melts mostly are known from theoretical modelling. It is in the magma-chambers and conduit systems at the mantle-crust transition that the parental melts are closest to their juvenile compositions. However, *in situ* studies of products and processes at these great depths of the continental lithosphere are very rare in deed. Particularly the origin, properties and significance of volatile-rich phases are lost during decompression from the deep lithosphere to the surface.

This knowledge-gap can be resolved by studying the few rare localities preserving lower crustal conduit system such as those preserved at Ivrea in NW Italy (Fiorentini et al. 2018) and the large volcanic conduit systems of the Seiland Igneous Province (SIP) in N. Norway (Fig. 1). SIP is the focus of this communication.

At the depths of SIP and Ivrea (Fiorentini et al. 2018) we are observing distinctive properties of melts, fluids and ore-deposits compared to the well-known equivalents at the shallow locations of LIP's. We observe a large range of enigmatic melt compositions, as well as mixing and un-mixing of diverse magmas and volatile phases and the formation and disruption or ore-deposits. It is clear that C-O-H-S volatile-rich phases here are omnipresent and highly enriched compared to shallow parts of LIP-forming systems (Fiorentini et al. 2018; Larsen et al. 2018). Arguably, it appears that volatile-rich melts aid in transporting dense ultramafic melts and in disrupting, mobilizing and upgrading PGE-Cu-Ni deposits.

2 The Seiland Igneous Province (SIP) – a giant volcanic conduit system

The Seiland Igneous Province (SIP) consists of >5,000 km^2 of mafic, ultramafic and alkaline melts that, for the majority of the intrusions, were emplaced into the lower continental crust (30-40 km's depth) in <10 Ma (570-560 Ma) and with alkaline as well as ultramafic magmatism spilling in to the L. Cambrian. As the SIP was a deep-seated conduit system co-forming with the Central Iapetus Magmatic Province (CIMP), it represents the deepest parts of CIMP, representing a key locality in which to study the ascent, emplacement and modification of dense mantle melts enroute to more shallow igneous systems. Here, in SIP, we may study igneous processes that relates to asthenosphere deep-lithosphere interaction processes prior to the melt-modifying processes that influence the parent melts during ascent towards the shallow crust.

Ultramafic complexes dominated by peridotitic cumulates occupy 1/3 of SIP and comprise the main volcanic conduits along which ultramafic magma migrated upwards in the continental lithosphere. The Reinfjord Complex is an excellent example of one of these conduit systems.

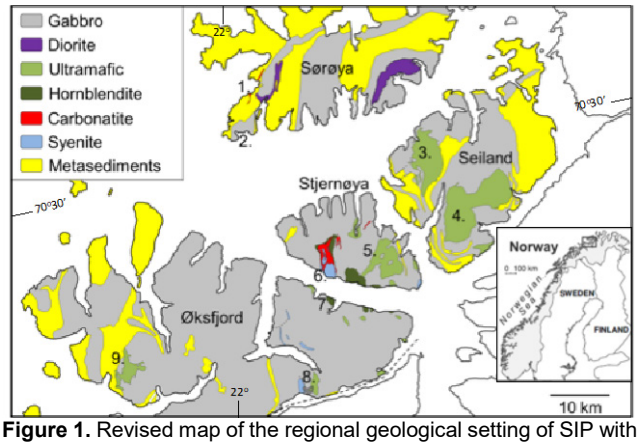

Figure 1. Revised map of the regional geological setting of SIP with main localities discussed in the text. (see Larsen et al. 2018 for detailed references) 1) Breivikbotn Carbonatite-Syenite Complex, 2) Hasvik Layered Gabbro, 3) Nordre Brumannsfjord UM-Complex, 4) Melkvann UM-Complex, 5) Kvalfjord UM-Complex, 6) Lillebukta Carbonatite-Syenite Complex, 7) Lokkarfjord Hornblendite (PGE-Cu-Ni deposits), 8) Tappeluft alkaline and UM-Complex, 9) Reinfjord UM-Complex (PGE-Cu-Ni deposits).

The ultramafic cumulates formed at the emplacement of picritic to komatiitic parental melts (16-22 wt% MgO) into layered gabbros in three major pulses (1-3 in Fig. 2) punctuated by several smaller replenishment events. The first two pulses, formed olivine-clinopyroxenite and wehrlite, comprising modally layered ol–cpx±opx cumulates. The final phase formed dunitic cumulates in the centre of the intrusion (Fig. 2). Phase 3 intruded into wehrlitic crystal-melt mushes. The dunite-forming melts assimilated wehrlitic cpx to form discordant replacive dunite bodies. Super-imposed upon these major events, cryptical zonation of ol and cpx reveals several replenishment episodes. We have identified 15 events over only 700 metres of cumulates. Field observations document smaller replenishment events of pyroxenitic melts. They occur as irregular dykes that intersect semisolid cumulates before dissipating in mushy melts higher up in the stratigraphy. One such event is associated with the formation of a 5 metres thick PGE-Ni horizons with 0.8 ppm Pt, Pd and Os. We also observe that the dunitic melt-mushes were infiltrated by several events of alkaline CO_2-H_2O rich melts forming globules and veinlets of feldspathoids, amphibole, carbonates, opx and cpx. The dunites contain several PGE-Cu-Ni rich horizons and it is clear that ore formation is associated with the formation of the dunitic cumulates.

Together, the rich diversity of igneous rocks documents the complexity of melts that are produced during plume assisted emplacements of very large volumes of mafic-ultramafic melts. Not least, in Reinfjord we learn to appreciate the importance of melt modification (mixing-assimilation etc.) of mantle derived melts in the deep crust before the “homogenized” products are emplaced in shallow magma chambers or flows.

3 Ore-forming processes in deep-seated giant magmatic conduit system

It was recently confirmed that SIP may have a significant ore-forming potential of Cu-Ni-PGE deposits (Schanche et al. 2012). Equally important for the formation of SIP, the ore-forming processes in the Reinfjord Complex document the importance of volatile fluxing of sulphur and carbon during emplacement of the ultramafic magmas (Nikolaisen 2016; Larsen et al. 2018), similar to observations in the Ivrea conduits (Fiorentini et al. 2018). Accordingly, minute but conspicuous assemblages of magmatic carbonate and sulphide are common throughout the Reinfjord Complex, particularly where Cu-Ni-PGE deposits occur.

Reinfjord also features *contact deposits* (Larsen et al. 2018) but the largest and richest deposits are hosted in the dunitic cumulates (Schanche et al. 2012; Larsen et al. 2018). Only the dunite hosted deposits are described here because of their clear economic potential.

3.1 Dunite hosted deposits

The largest deposits appear as a 5 Ohm conductor providing an excellent contrast to the 3000 Ohm Central Series dunitic cumulates (Schanche et al. 2012). Modelling implied a conformable saucer-shaped body at a depth of c. 40 to 100 metres covering an area of 600 x 400 metres. A late magmatic normal fault runs through the centre of the deposit and downthrow the eastern block 50-60 metres. Exploratory drilling confirmed the presence of weakly disseminated deposits at 85 and 110 m (eastern block) below the surface with 1.6 and 1.2 wt% total sulphides, respectively. Here, the upper reef comprises 5 metres of dunite with an average of 0.4 wt% sulphide-bound Ni, 0.14 wt% Cu and 70 ppb PGE+Au whereas the lower reef comprises 5 metres with 0.23 wt% Ni and 715 ppb PGE+Au. Importantly, most of the PGE+Au is confined to a 1 m dunite section with 1635 ppb PGE+Au including 750 ppb Pd, 430 ppb Pt, 220 ppb Au and, 235 ppb IPGE with an Os-peak at 200 ppb. The Ni peak actually occurs 7 metres higher up, hence the PGE-reef is clearly decoupled from the Ni-reef and the Ni-reef is decoupled from the Cu-reef. Mineralogically, c. 50 % of the sulphides are pentlandite and chalcopyrite, the remaining part being pyrrhotite. Detailed studies demonstrated that peak values are associated with dunitic cumulates belonging to the third major recharge event (Nikolaisen, 2016; Larsen et al. 2018).

The sulphide rich horizons were also discovered in two recent (RF-3 and 4 on Fig. 2) drill holes sampled c. 600 metres north of the two discovery holes. Here, the deposits occur from 40-80 metres below the surface in the dunites. Cu peaks with values of c. 0.1 wt % Cu in two 10 m thick reefs separated by 20 metres of dunite (Fig. 9). Finally, there is a deep-seated Cu-horizon at 349 m with 0.1 wt% Cu over 20 metres occurring at the transition between dunites and pyroxenites (RF-4 in Fig. 2).

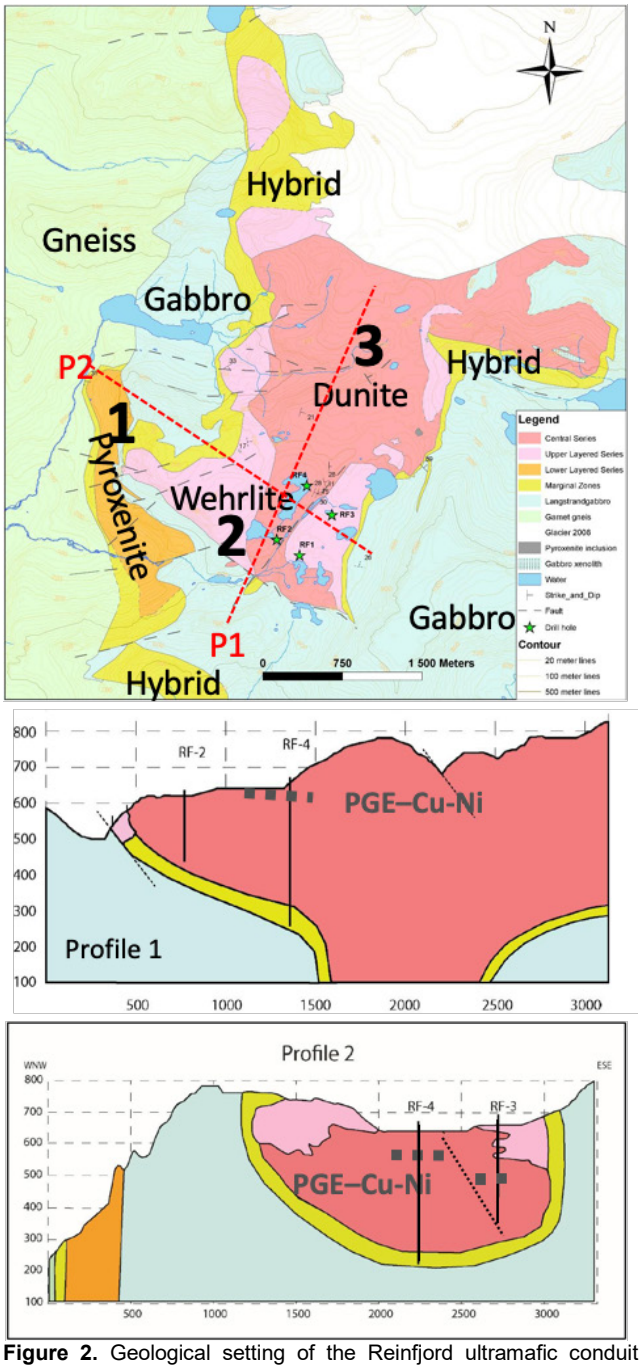

Figure 2. Geological setting of the Reinfjord ultramafic conduit showing main igneous lithologies, position of drillholes (RF-1 to RF-4) and location of the main Cu-Ni-PGE deposit. 1-3 marks the three main recharge events forming the Reinfjord Complex.

The PGE deposit contain 0.3 ppm PGE over 5 metres and is decoupled from the Cu-deposits in occurring at 64 metres between the two Cu-maxima. None of the Cu deposits are associated with significant Ni-sulphide anomalies. The highest Ni values occur 5 metres above the PGE-horizon.

There are 4 more PGE horisons with c. 0.1 ppm PGE, but none of them are close to the Ni and/or Cu sulphide deposits.

It is clear that the main PGE-horizons are decoupled from both Cu and Ni horizons, and that the Ni-horizon, that occur 5 and 7 metres above the PGE's, is Cu-poor. Furthermore, PGE deposits coincide with relatively Sulphur poor segments of the igneous stratigraphy.

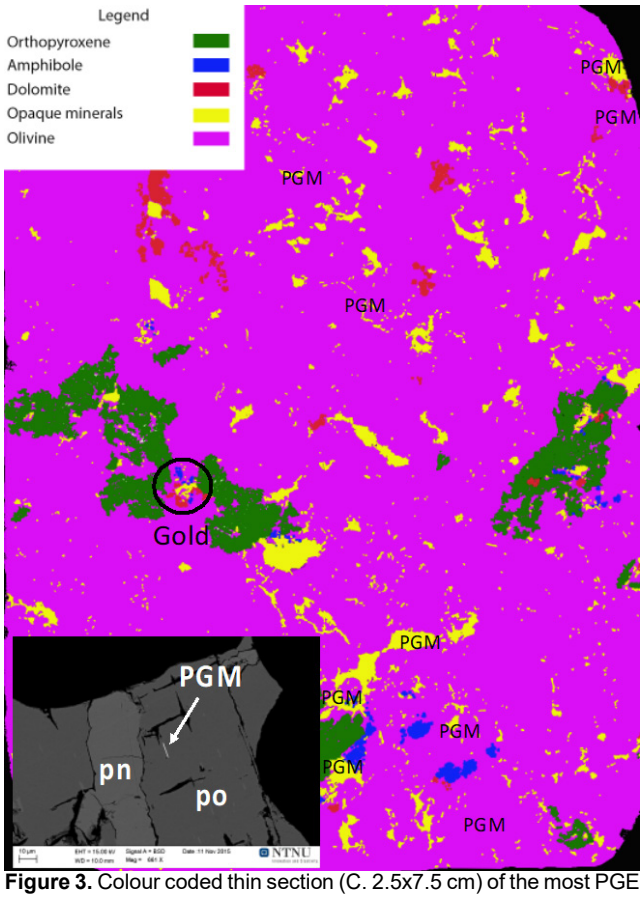

Figure 3. Colour coded thin section (C. 2.5x7.5 cm) of the most PGE rich parts of the RF-1 drill-core. Minerals are colour coded. Note that opaque minerals are Cu-Ni-Fe sulphides. PGM denotes Platinum Group Minerals, mostly Moncheite and Mereskyite. The relatively high abundance of dolomite (red) and amphibole (blue) is evident. Insert in left image, show the close association of Pt-Te minerals with exsolutions of pentlandite (pn) in pyrrhotite (po) tenors. See main text for more information.

The Pt/Pd ratios at all anomalous horizons in the drill-cores are between 1:1 and 1:2 whereas, "barren" sections have an average of 2:1. The PPGE/IPGE ratios are comparable to the Merensky Reef (S. Afr. Rep.) with typical values of 2-10. Platinum Group Minerals (PGM) are dominated by tellurides mostly *Moncheite* ((Pt, Pd)Te_2) and *Merenskyite* ((Pd, Pt)(Bi, $Te)_2$) whereas Au varies from pure gold to electrum with 40 % Ag (Nikolaisen 2016; Larsen et al. 2018). However, we also found several IPGE minerals including *hollingworthite* ((Rh,Ir,Os,Pt)AsS) and *irarsite* ((Rh, Ir)AsS_2).

Most of the PGMs occur together with sulphides that are commonly intimately intergrown with pentlandite exsolution in pyrrhotite (Fig. 3), whereas gold-rich phases show a close association with carbonate-sulphide assemblages (Nikolaisen 2016; Larsen et al. 2018). Similarly, the PGE-mineralised sections normally contain high concentrations of carbonates and hydrous minerals (Fig. 3) that we have interpreted to represent alkaline melts that co-existed with the ultramafic melts that formed

the dunitic cumulates and/or, alternatively, were dissolved in the ultramafic parental melts prior to the formation of the dunitic cumulates.

In situ ion probe sulphur isotope analysis of sulphides yielded bulk $\delta^{34}S$ values around -2 to +2 ‰ for dunite hosted deposits as well as for sulphides in barren parts of the dunites whereas the host gabbro and paragneisses gave average values of +4 ‰ and +11 ‰, respectively (Larsen et al. 2018). Accordingly, the parental melts forming the ultramafic cumulates gained its sulphur from a distinctively different source region than both the paragneisses and the layered gabbros.

4 Origin and significance of PGE-Cu-Ni deposits in lower crustal conduit systems

Our studies at the Seiland Igneous Province is a rare probe in to the igneous processes pertaining to the deep-seated parts of a LIP-forming igneous system. An important lesson is that the diversity and composition of juvenile igneous melts is considerably more complex than the upper crustal formations of LIP-magmatism may imply. Not least, in SIP, we observe that ultramafic melts of picritic/komatiitic composition are close to or at sulphide saturation, are emplaced in the lower crust together with alkaline carbonated hydrous-rich melts and are themselves enriched in volatiles.

This is comparable to observations from the Ivrea Zone in NW Italy, where the parental melts forming deep-seated (c. 0.8 Gpa) conduit systems are also enriched in volatile constituents and show a characteristic alkaline signature (Fiorentini et al. 2018). The Ivrea conduits are also enriched in Cu-Ni-PGE mineralized sulphides and with an average of +1.35 ‰, the $\delta^{34}S$ values fall in the same range as at SIP and support that the likely isotopic range for the sub continental mantle is a narrow interval close to nil (Fiorentini et al. 2018).

The genesis of the sulphide deposits in the Reinfjord conduit system involves liquid immiscibility of a sulphide liquid at or shortly after emplacement of the dunite forming melts. The irregular distribution of the sulphides, sometimes over 10-20 metres of cumulates at several horizons in the dunites, imply multiple episodes of deposition and remobilisation in an open conduit system exposed to repetitive recharge events. The PGE-rich horizons are sulphide poor (<1 wt.% S) and decoupled from the Cu-Ni maxima. Contrary to the Cu-Ni-rich horizons, the PGE-rich zones are narrow occurring over only 1-2 metres of the cumulate stratigraphy.

Apparently, most of the PGE-Cu-Ni deposits at Reinfjord occur in a swelling structure forming a side chamber along the main conduit (Fig. 2, profile 1 and 2). Arguably, potential deposits forming in the actual conduit may have been remobilised hence migrated towards higher crustal levels.

Finally, we have the high contents of carbonates and hydrous phases throughout all cumulate types as well as in early and late dykes, i.e. it may be concluded that mafic as well as ultramafic parental melts were strongly enriched in dissolved volatile constituents.

The significance of the volatile-rich phases for asthenosphere-lithosphere transfer of mafic-ultramafic melts and ore-forming processes is not currently resolved. However, the fact that both SIP and the Ivrea conduits (Fiorentini et al 2018) show a high abundance of *volatile-rich* phases indicates that mafic-ultramafic melts in the deep-seated parts of volcanic conduit-systems may be the norm rather than an anomaly. During decompression towards the surface, this volatile-rich signature may be lost when the carbonate-component becomes immiscible in the silicate melts under the formation of shallow alkaline complexes.

Acknowledgement

Generous funding from the Nordic Council of Ministers, the Directorate for Internationalisation in Higher Education (DIKU) and NTNU made this study possible. Inspiring reviews from Prof. Fiorentini are highly appreciated.

References

Cox, K., (1980) A model for flood basalt vulcanism. Journal of Petrology, 21:629-650

Ernst, R.E., Bell, K. (2010) Large igneous provinces (LIPs) and carbonatites. Mineralogy and Petrology, 98:55-76

Fiorentini, L. M., LaFlamme C, Denyzyn S., Mole D., Maas R., Locmelis M., Caruso S., Bui T. (2018) Post-collisional alkaline magmatism as gateway for metal and sulfur enrichment of the continental lower crust. Geochimica et Cosmochimica Acta 223:175–197

Larsen R.B., Grant T., Sørensen B.E., Tegner C., McEnroe S., Pastore Z., Fichler C., Nikolaisen, E., Grannes K.R.B., Church N.S., ter Maat G., Michels A. (2018) Portrait of a giant deep-seated magmatic conduit system: The Seiland Igneous Province. Lithos, 266-299

Nikolaisen, E., 2016. Platinum Group Elements in the Reinfjord Ultramafic Complex (Master's thesis, NTNU).

Schanche, M., Iljina, M., Larsen, R.B., 2012. New Nickel-Copper-Platinum Group Element Deposits in N. Norway. Mineralproduksjon 2:91-99.

Ni-Cu-(PGE) fertility of the Zambezi belt rift magmatism: source and temporal controls

Ward A. Laura, Holwell A. David
School of Geography, Geology and the Environment, University of Leicester, UK

Tapster Simon
NERC Isotope Geosciences Laboratory, British Geological Survey

Abstract. Magmatic Ni-Cu-(PGE) sulphide deposits are the world's most valuable source of Ni and PGEs. It is widely recognised that many major Ni-Cu-(PGE) sulphide deposits are spatially associated with craton or palaeocraton margins; a surface manifestation of the channelisation of plume magmas into zones of thinning lithosphere. Whilst many aspects of the ore system are well-constrained, the occurrence of mineralised and unmineralised intrusions within the same geological setting cannot yet be adequately explained. Understanding why unmineralised intrusions form within otherwise prospective terrains is the 'holy grail' of the Ni exploration industry and highlights a number of substantial research challenges. This study represents the first of its kind in the Zambezi belt in testing the temporal and isotopic characteristics of a suite of mineralised and unmineralised intrusions along this prospective belt. Using high precision dating techniques (CA-ID-TIMS) and a range of isotopic tracers (Lu-Hf, Sm-Nd, Rb-Sr), a suite of variably mineralised intrusions from the Zambezi belt are assessed in order to try and better understand the interplay between magma fertility and geodynamic controls.

1 Introduction

Magmatic Ni-Cu-(PGE) sulphide deposits represent some of the world's most valuable metal accumulations, accounting globally for ~56% of Ni and ~96% of PGE production. Many of the world's largest and most lucrative Ni-Cu-(PGE) deposits exhibit a well-defined spatial relationship with craton margins (e.g. Voisey's Bay, Noril'sk, Jinchuan; Begg et al. 2010). In fact, there are few major Ni-Cu-(PGE) deposits for which there is no documented relationship (Begg et al. 2010; Maier and Groves 2011). Based on this observation, these regions are frequently targeted as corridors of enhanced prospectivity. Craton margins comprise zones of relatively thin lithosphere which become focal points for regional strain during tectonism, creating points of dilation along former deep-rooted fault systems (Begg et al. 2010; Barnes et al. 2015). Llarge and sustained magma volumes are able to ascend through these established crack networks, becoming channelised in the upper crust into high-flux magma conduits: prime conditions for ore genesis (Barnes et al. 2015; Lightfoot and Lamswood 2015). Particularly well-mineralised cratons include those in central-southern Africa (e.g. Kaapvaal, Zimbabwe and Congo cratons), though some are seemly more PGE (e.g. Kalahari) than Ni-Cu rich (e.g. Congo; Maier and Groves 2011).

The ore-forming processes responsible for Ni-Cu-(PGE) sulphide mineralisation are relatively well constrained. The generally supported hypothesis is that parental ultramafic-mafic magmas must saturate with sulphide in the near surface environment (Naldrett 1999). The magmatic plumbing networks which feed these systems need to sustain dynamic magma flows in order to successfully scavenge chalcophile elements from their parental melts and upgrade metal tenors to economic concentrations. Whilst process models for Ni-Cu-(PGE) mineralisation are seemly robust, less understood are the province/ regional geodynamic controls on magma fertility *before* the influences of shallow upper-crustal interactions. This point is largely founded on the observation that within a number of well-explored terrains, mineralisation is unevenly distributed amongst superficially similar intrusions. For example, in the Voisey's Bay district, northern Canada, the Voisey's bay intrusion hosts a giant ore-body whilst the apparently similar surrounding intrusions are sub-economic. Likewise, in the Yunnan and Sichuan Provinces of SW China, a number of heavily mineralised intrusions are surrounded by superficially similar intrusions, containing sub-economic to uneconomic accumulations of low tenor sulphide (Lightfoot and Lamswood 2015).

A substantial challenge to research and exploration lies in understanding the cryptic processes resulting in the occurrence of unmineralised intrusions in otherwise prospective regions. Using a suite of variably mineralised (economically mineralised, weakly mineralised, unmineralised) mafic-ultramafic intrusions from across the Zambezi belt, southern Zambia, this study aims to investigate the geodynamic and temporal influences on regional magma fertility and how these relate to the source and source characteristics of a deposit prior to the influences of upper crustal processes/interactions.

2 Case study area: The Zambezi belt

The Zambezi belt represents an example of a classic continental rift system and hosts abundant mafic-ultramafic rift magmatism, including the economic Munali Ni deposit. The Zambezi belt forms a key component in the network of Neoproterozoic tectonic belts in central-southern Africa that formed during the amalgamation of the supercontinent Gondwana (Johnson et al. 2007).

2.1 Geochronology of the Zambezi belt

The Zambezi metamorphic belt is situated between the

Congo-Kalahari cratons and forms part of the Pan-African orogenic system (Johnson et al. 2007). The Neoproterozoic Zambezi belt is characterized by abundant mafic-ultramafic magmatism exclusively hosted in high-level basin sediments as outlined in the classic 'craton-margin' setting defined by Begg et al (2010). The belt is comprised of sediments belonging to the Zambezi Supracrustal sequence (ZSS), which are largely made up of sedimentary, volcanic and volcanoclastic rocks unconformably resting on a basement of gneiss (~1106 Ma) and granite (~1090 Ma). They are thought to represent a full tectonic cycle from continental rifting to subduction (Vinyu et al. 1999; Johnson et al. 2007).

Johnson et al. (2007) constrained much of the temporal evolution of the Zambezi basin where the onset of continental rifting and sedimentation is constrained by basal rhyolite flows as clasts in conglomerates at the base of the overlying ZSS units. A maximum depositional age of the ZSS at 879 ± 19 Ma has been proposed (Johnson et al. 2007). The main phase sedimentation is thought to have ceased by 820 Ma, marked by the emplacement of two geochemically similar A-type granitoids (820 ± 7 Ma Ngoma Gneiss and 821 ± 9 Ma Lusaka granite). Whilst the exact tectonic implications of the emplacement of these granitoid bodies is yet to be fully established, they are thought to mark the final stages of basin development and onset of basin convergence (Katongo et al. 2004; Johnson et al. 2007).

2.2 Mafic magmatism in the Zambezi belt

The Zambezi belt is characterised by hundreds of superficially similar mafic-ultramafic intrusions emplaced into a common stratigraphic succession within the Zambezi belt stratigraphy, independent of the degree of mineralisation. The Munali Intrusive Complex (MIC) is hosted within the upper carbonate sequences of the ZSS and comprises two main units: the Central Gabbro unit (CGU) and the Mafic-Ultramafic-Breccia-Unit (MUBU; Fig. 1). High-precision CA-ID-TIMS U-Pb dating of zircons from the Munali CGU and MUBU yields ages of 857 ± 0.84 Ma and 857 ± 1.9 Ma, respectively, and thus likely correlate with emplacement during early stages of basin extension and rifting (Holwell et al. 2017). Associated with the MIC are several, apparently similar intrusions (*Chikani, Chibuku, Termite and T1B; see Fig.1*) thought to be genetically related to the MIC based on spatial associations and whole rock geochemistry. The Chibuku, Termite and T1B intrusions are known to contain Ni-sulphide mineralisation, though to what economic extent is still to be established. Dating of the Chibuku intrusive body in this study suggests emplacement occurred around ~855 Ma, strengthening the genetic association with the MIC and early extensional relationships.

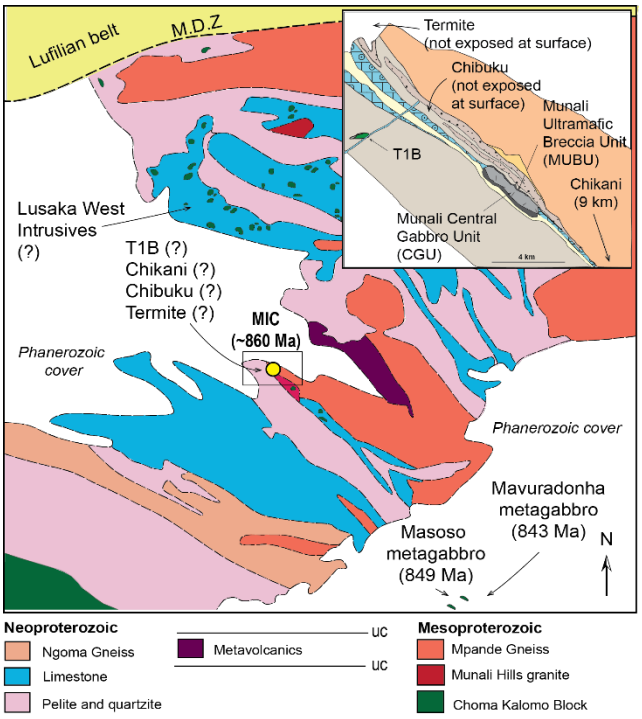

Figure 1. Map of the Zambezi Supracrustal Sequence and location of the Lusaka West intrusions and MIC. Insert map of the MIC and surrounding intrusions (Chibuku, T1b, Termite, Chikani).

Fifty five kilometers NE of the MIC are the Lusaka West intrusives (Fig. 1), which appear both superficially and geochemically similar to the Munali Ni-Cu-(PGE) deposit. The Lusaka West intrusions comprise numerous small differentiated mafic-ultramafic intrusions emplaced into the same meta-sedimentary succession as the MIC, ranging from sub- to uneconomic. Whilst some of the Lusaka West intrusions show evidence of localised sulphide segregation based on whole rock Cu/Zr ratios, no primary-magmatic Ni-sulphides are observed and PGE concentrations are around that of average mantle compositions.

Traditionally, these intrusions have been assigned either a Pan-African (~520 Ma) or Munali (~860 Ma) emplacement age. However, high precision dating conducted in this study suggests intrusions are much older (~737 Ma), around 100 Ma prior to peak Pan-African metamorphism in the Zambezi belt, and ~123 Ma younger than Munali emplacement, overlapping with reported magmatism in the Copperbelt.

2.3 Preliminary findings and further work

Preliminary data currently alludes to a temporal distinction between the apparently fertile Munali hills and barren Lusaka West intrusives. We suggest that is during discrete early extensional phases of the Zambezi basin evolution (~880 to ~820 Ma) that magmatism was particularly capable of segregating economic accumulations of sulphide. Furthermore, data suggest that later intrusion emplacement during periods of regional convergence (after ~820 Ma) are seemly less

fertile. The source characteristics of these temporally distinct episodes will be assessed using isotopic tracers to reconstruct the 4D evolution of Ni-Cu-(PGE) mineralisation in craton margin settings. We aim to continue testing the hypothesis that the geodynamic evolution of the Zambezi Mobile Belt exerted a fundamental control over magma fertility, with a view to framing findings in the context of basin evolution and potential magma sources.

Acknowledgements

The management and staff at Mabiza Resources and Consolidated Nickel Mines are thanked for their technical and logistical support during fieldwork in Zambia.

References

Barnes SJ, Cruden AR, Arndt N, Saumur BM (2016) The mineral system approach applied to magmatic Ni–Cu–PGE sulphide deposits. Ore Geology Reviews 76: 296-316.

Begg GC, Hronsky JA, Arndt NT, Griffin WL., O'Reilly SY, Hayward N (2010) Lithospheric, cratonic, and geodynamic setting of Ni-Cu-PGE sulfide deposits. Economic geology 105:1057-1070.

Holwell DA, Mitchell CL, Howe GA, Evans DM, Ward LA, & Friedman, R (2017) The Munali Ni sulfide deposit, southern Zambia: A multi-stage, mafic-ultramafic, magmatic sulfide-magnetite-apatite-carbonate megabreccia. Ore Geology Reviews, 90: 553-575.

Johnson SP, De Waele B, Evans D, Banda W, Tembo F, Milton JA, Tani K (2007) Geochronology of the Zambezi supracrustal sequence, southern Zambia: a record of Neoproterozoic divergent processes along the southern margin of the Congo Craton. The Journal of Geology 115: 355-374.

Katongo C, Koller F, Kloetzli U, Koeberl C, Tembo F, De Waele B (2004) Petrography, geochemistry, and geochronology of granitoid rocks in the Neoproterozoic-Paleozoic Lufilian–Zambezi belt, Zambia: Implications for tectonic setting and regional correlation. Journal of African Earth Sciences 40: 219-244.

Lightfoot PC, Evans-Lamswood D (2015) Structural controls on the primary distribution of mafic–ultramafic intrusions containing Ni–Cu–Co–(PGE) sulfide mineralization in the roots of large igneous provinces. Ore Geology Reviews 64: 354-386.

Maier WD, Groves DI (2011) Temporal and spatial controls on the formation of magmatic PGE and Ni–Cu deposits. Mineralium Deposita, 46: 841-857.

Naldrett AJ (1999) World-class Ni-Cu-PGE deposits: key factors in their genesis. Mineralium deposita 34: 227-240.

Vinyu ML, Hanson RE, Martin MW, Bowring SA, Jelsma HA, Krol MA, Dirks PH (1999) U–Pb and 40Ar/39Ar geochronological constraints on the tectonic evolution of the easternmost part of the Zambezi orogenic belt, northeast Zimbabwe. Precambrian Research 98: 67-82.

Insights into the origin of the Munali magmatic sulfide deposit: evidence for a hidden Cu orebody?

Daryl Blanks, David Holwell
University of Leicester, UK

Stephen Barnes, Louise Schoneveld
CSIRO Mineral Resources, Perth, Australia

Abstract. The Munali magmatic sulfide complex is an enigmatic mafic-ultramafic breccia deposit, comprised of atypical Cr-poor magmatic host rocks and an unusual Ni rich/Cu-poor carbonate-apatite-magnetite sulfide assemblage. Mineralisation is present as a sulfide matrix breccia, in which the clasts are present as an array of lithologies and sizes ranging from < 0.5 cm to > 5 m and is mined principally for its Ni resource, with Cu, PGE and Co as supplementary by-products. Several mineralisation styles have been identified which contain a similar sulfide mineralogy (pyrrhotite >> pentlandite > chalcopyrite ± pyrite), but display differences in sulfide abundance, gangue mineralogy and geochemical characteristics. Additionally, variations of Pd and Co within pentlandite and pyrite between the styles, suggest complexities in emplacement timing and/or sulfide melt interactions. The bulk sulfide at Munali displays high Ni/Cu ratios and an extreme negative Au anomaly, which is atypical for a mafic-ultramafic complex. Therefore, Munali may represent a sulfide system where the primary sulfide melt that crystallised was unusually low in Cu and Au or may instead suggest that syn-to-post magmatic processes may have altered or displaced the Cu(-Au)-rich component of the orebody and that these may now reside elsewhere in the system.

1 Introduction

The Munali magmatic sulfide deposit is a highly complex Neoproterozoic Ni-Cu-Co-PGE mafic-ultramafic breccia located within the Zambezi Belt in southern Zambia.

The deposit represents a multi-phase dynamic system comprised of an early unmineralised gabbroic core, surrounded by a later marginal mafic-ultramafic breccia unit that is host to a sulfide matrix (Holwell et al. 2017). The mafic-ultramafic breccia clasts in this unit comprise dolerite, weakly mineralised poikilitic gabbro and a suite of atypical ultramafic rocks that include olivinite (Cr-poor olivine cumulates) and phoscorite (olivine-magnetite-apatite rock). The intrusive complex is steeply dipping and exhibits typical characteristics of a magmatic-conduit system located along a translithospheric fault zone. Mineralisation is open at depth with the ore zone comprised of a massive sulfide breccia ore composed of an unusual Ni-rich but Cu-poor sulfide assemblage with associated carbonate-apatite-magnetite. The carbonate is of mantle origin and has carbonatitic affinities that are consistent with the presence of phoscorites.

2 Sulfide characteristics

The sulfide matrix of the mafic-ultramafic breccia forms the main stage of mineralisation with the sulfide comprised of multiple styles, characterised by differences in sulfide abundance, ore and gangue mineralogy and textural associations and include:

1) Massive sulfide;
2) Semi-massive sulfide;
3) Semi-massive sulfide with apatite;
4) Apatite-rich pyritic sulfide;
5) Carbonate-rich sulfide;
6) Talc-carbonate associated sulfide.

All styles comprise the typical magmatic sulfide assemblage of pyrrhotite, pentlandite, and chalcopyrite ± pyrite and magnetite in variable abundances. Geochemically, the sulfides are very primitive, Fe-rich monosulfide solid solution (mss) cumulates with variable Pt/Pd ratios that are nearly always < 1, with a high Ni/Cu ratio of approximately 7.5 to 10 (Fig. 1). As a result of the low Cu tenor, the sulfide at Munali plots towards the lowest extent for the mafic associated field and overlaps with the field for sulfides associated with komatiite magmatism.

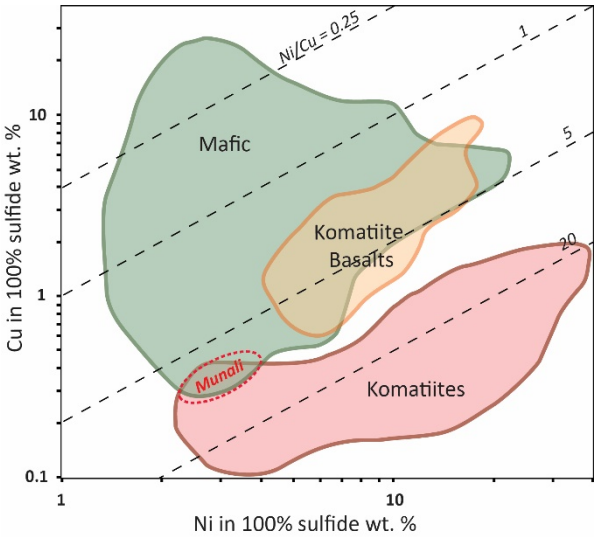

Figure 1. Ore compositions and bulk metal tenors of Cu and Ni in 100% sulfide showing the fields for mafic, komatiite, komatiite basalts and the red field for Munali, exhibiting a Ni/Cu ratio of around 7.5 to 10 (after Barnes et al. 2017).

Massive and semi-massive sulfide (mineralisation styles 1 and 2), represent the most voluminous sulfide styles of the ore-body and exhibit the lowest Cu tenors. In contrast, styles 3, 4 and 5, where mineralisation is associated with gangue minerals apatite and carbonate, display relatively high Cu tenors.

Sulfides display striking loop textures, comprising pentlandite and lesser chalcopyrite forming continuous rims around pyrrhotite crystals. These are very similar to textures observed in the Nova deposit (Barnes et al. this volume) and are interpreted similarly as the result of peritectic growth of high-T pentlandite from residual sulfide liquid.

Platinum-group mineral (PGM) assemblages are present almost exclusively as Pd>Pt tellurides, with slight variations between styles. PGMs are present solely as Pd-tellurides in the apatite and carbonate styles whereas massive to semi-massive sulfide without these gangue appear to show much more variable mineralisation of Pd>Pt tellurides as merenskyite, monchiete, kotulskite and rare sperrlyite. Notably, no Au-bearing minerals have been identified.

2.1 Sulfide geochemistry

The concentrations of PGE and other chalcophile elements have been determined by laser ablation-inductively coupled plasma-mass spectrometry (LA-ICP-MS) in pyrrhotite, pentlandite, chalcopyrite and pyrite from all mineralisation styles, where present. Although Pd is present as Pd-tellurides associated with sulfide, there are significant levels of Pd hosted in solid solution in pentlandite, ranging from < 1 to 500 ppm, whilst Pt, not present in significant quantities as PGMs was not found to be elevated in any of the sulfides analysed. The high Pd content of the loop-textured pentlandite is evidence for its peritectic origin (Mansur et al. 2019).

No Co-minerals have been identified as part of the base metal sulfide mineral assemblage, although Co is an economic by-product of the deposit. Cobalt is instead present in notable quantities (up to 4 wt. %) within pentlandite and pyrite where four major trends have been identified that include 1) a positive correlation of Ni and Co in pentlandite; 2) high Co with low Ni in pentlandite associated with semi-massive sulfide with apatite; 3) high Co in pyrite and 4) moderate Co in As and Ni enriched pyrite hosted within talc-carbonate associated sulfide, with the latter likely formed from later hydrothermal enrichment during talc-carbonate formation. No Co was present in notable quantities within chalcopyrite and pyrrhotite in any style. Additionally, Au was not detected in solid solution within pyrrhotite, whilst several analyses detected low Au in pyrite, chalcopyrite and pentlandite (< 0.03 ppm) most were below detection limit.

2.2 PGE Geochemistry

Bulk PGE profiles from the different mineralisation styles at Munali highlights two key trends within the sulfide (Fig. 2). Massive sulfide and semi-massive sulfide without carbonate and/or apatite show a moderate steepening trend from IPGE to PPGE with an average (Pd/Ir)N ratio of 265. Sulfide associated with apatite and carbonate appear relatively more fractionated with an average (Pd/Ir)N ratio of 3374, and is slightly more enriched in Cu. However, although overall the system appears to be fractionated with respect to the PGE, there is a distinct negative Au anomaly along with relatively low Cu contents in the system.

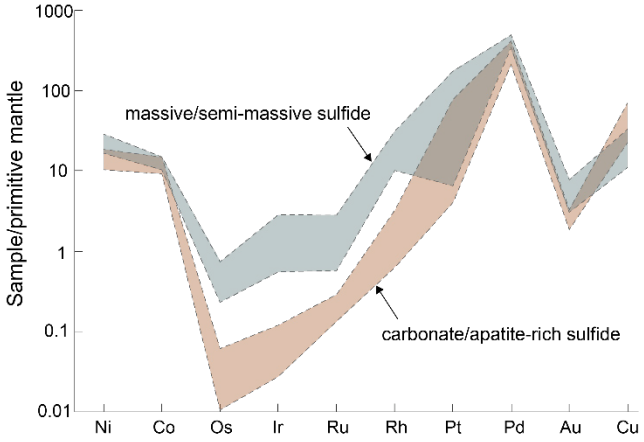

Figure 2. Primitive mantle normalised bulk PGE profiles for the main sulfide mineralisation styles.

3 The loss of Cu?

The sulfide at Munali represents a magmatic system that is depleted in Cu and Au in relation to similar deposits worldwide, representing an unusual, fractionated Cu-poor sulfide system, with moderate to high Pd/Ir and high Ni/Cu ratios. As such, this may indicate that the Cu-poor nature of the orebody may reflect an inherent characteristic of the initial sulfide liquid composition, representing a sulfide system retaining the mss cumulate portion. This may be due to sulfide at Munali reflecting a new subclassification of sulfide mineralisation systems, potentially linked to phoscoritic/carbonatitic magmas.

However, it is possible that the Cu and Au depletion may be due secondary processes and does not represent the primary sulfide liquid composition. Although the sulfide is Cu-poor, there is textural evidence for Cu-rich sulfide liquid migration within the deposit on a cm scale, whereby chalcopyrite is present within cracks and fractures in the brecciated host rocks. As such, it may be possible that on a larger scale, the Cu portion of the orebody, which may be additionally enriched in Au and PGE, may have migrated via pre-existing structures or as a result of syn- to post-tectonic processes. Thus, there remains the possibility of discovering a Cu-rich portion of the orebody a depth.

An alternative explanation may be that hydrothermal fluids interacted with the sulfides and stripped them of their most mobile metals such as Cu and Au via, for example, Cl-rich fluids (Aird and Boudreau 2013; Hanley et al. 2005). These may have been meteoric and derived from evaporitic sediments (for which there is evidence in the immediate host rocks), or magmatic-metamorphic in origin, due to the depletion in both Au and Cu within the orebody.

Overall, Munali represents an enigmatic deposit with unusual host rocks, gangue mineralogy and sulfide composition. These associations could represent primary features and a new style of magmatic sulfide deposit, or may be indicative of another process involving the modification of the sulfide mineralisation during or post emplacement.

Acknowledgements

DB was funded by Consolidated Nickel Mines and the University of Leicester. This work is additionally funded by NERC SoS Minerals consortium grant NE/M010848/1 "TeaSe: tellurium and selenium cycling and supply" awarded to the University of Leicester. Consolidated Nickel Mines are gratefully acknowledged for financial and logistical field support and permission to carry out and present this research.

References

Aird HM, Boudreau AE (2013) High-temperature carbonate minerals in the Stillwater Complex, Montana, USA. Contrib Mineral Petrol 166:1143-1160.

Barnes SJ, Holwell DA, Le Vaillant M (2017) Magmatic sulfide ore deposits. Elements 13:91-97.

Barnes SJ, Taranovic V, Miller JM, Beresford SW, Rennick S (2019) Sulfide-silicate textures and emplacement mechanisms of the Nova-Bollinger ores, Fraser Zone, Western Australia, this volume.

Hanley JJ, Mungall JE, Pettke T, Spooner ETC, Bray,CJ (2005) Ore metal redistribution by hydrocarbon-brine and hydrocarbon-halide melt phases, North Range footwall of the Sudbury Igneous Complex, Ontario, Canada, Mineralium Deposita 40:237-256.

Holwell DA., Mitchell CL, Howe GA, Evans DM, Ward LA, Freidman R (2017) The Munali Ni sulfide deposit, southern Zambia: a multi-stage, mafic-ultramafic, magmatic sulfide-magnetite-apatite-carbonate megabreccia. Ore Geol Rev 9:553-557.

Mansur ET, Barnes SJ, Duran CJ (2019) Textural and compositional evidence for the formation of pentlandite via peritectic reaction: Implications for the distribution of highly siderophile elements. Geology 47:351-354.

Fluorine and PGE-Au elevated signature of alkaline magmas from the Yilgarn Craton: insights into mantle fertility

Eunjoo Choi, Marco Fiorentini
Centre for Exploration Targeting, ARC Centre of Excellence in Core to Crust Fluid Systems (CCFS), University of Western Australia

Andrea Giuliani
KiDs (Kimberlites and Diamonds), School of Earth Sciences, University of Melbourne

Stephen Foley
ARC CCFS, Department of Earth and Planetary Sciences, Macquarie University

Abstract. Our current understanding of the nature of the mantle, under the Archean Yilgarn Craton, Western Australia is predominantly based on the image provided by a number of geophysical datasets and on the radiogenic isotope (e.g., Lu-Hf, Sm-Nd) composition of granitoid and ultramafic rocks. The PGE-Au signature of deeply sourced alkaline magmas may provide key insights into the metallogenic fertility of the mantle underlying the Yilgarn Craton. The Yilgarn Craton contains various types of alkaline rocks, including calc-alkaline lamprophyres (CAL), ultramafic lamprophyres (UML), carbonatites, orangeites and kimberlites. The PGE patterns of the CAL exhibit elevated $(Pd/Ir)_N$ ratios, whereas the other rock types are characterised by less fractionated PGE patterns, with lower $(Pd/Ir)_N$ ratios. In general, most alkaline magmas from the Yilgarn Craton appear to be anomalously enriched in Au. Furthermore, their key constituent magmatic minerals, such as amphibole, mica and apatite are anomalously enriched in F, and S. These volatiles may play a crucial role in the transport and concentration of precious metals from the mantle into the crust, contributing to explaining its exceptional metal endowment.

1 Introduction

The Yilgarn Craton in Western Australia is a world-class metallogenic Archean craton hosting considerable metal resources, including komatiite-associated Ni-sulfides and orogenic Au. Interest in the geodynamic evolution of the crust and upper mantle in the craton has increased greatly over the last decade through various studies, which mainly relied on regional scale geophysical datasets, as well as geochemical, isotopic and geochronological information of subalkaline felsic, mafic and ultramafic magmas (e.g. Blewett et al. 2010; Mole et al. 2013). However, these studies provided limited information on the composition of the lithospheric mantle, which may hold the key to understanding the exceptional metal endowment of this craton (Griffin et al. 2013).

This knowledge gap may be at least partially addressed through the study of the metal and volatile nature of a serious of poorly characterised alkaline magmas, which are distributed throughout the eastern part of the Yilgarn Craton as well as along its northern and southern margins. This study represents the first comprehensive characterisation of the precious element signature of alkaline magmas in this craton.

2 Geological Settings

2.1 Evolution of the Yilgarn Craton

The Yilgarn Craton mainly consists of metavolcanic and metasedimentary rocks, granitoid complexes, and greenstone belts, which formed principally between ~3050 and 2600 Ma, with minor older components >3700 Ma in age (e.g., Wilde et al. 1996; Myers 1995; Pawley et al. 2012; Griffin et al. 2004). It can be subdivided into the Western Yilgarn and Eastern Goldfields Superterrane based on stratigraphic, structural, geochemical and geochronological data, each comprising a number of domains, terranes and superterranes (Cassidy et al. 2006). The Eastern Goldfields Superterrane dominantly consists of ~ 2710-2690 Ma tholeiitic and komatiitic units and the ~2690-2660 Ma felsic volcaniclastic units (e.g., Cassidy et al. 2006; Barley et al. 2003). Craton-wide felsic magmatism from ~2650 to 2620 Ma is thought to reflect the cratonisation of the Yilgarn Craton into its current form and size (Cassidy et al. 2006; Czarnota et al. 2010; Mole et al. 2014).

2.2 Alkaline rocks in the Yilgarn Craton

The Yilgarn Craton contains various types of alkaline magmas, including CAL, UML, carbonatites, orangeites, and kimberlites. The spatial distribution of the alkaline rocks in the craton can be subdivided into three groups. The alkaline rocks on the northern boundary of the craton comprise orangeites and kimberlites with ages of 1324 ± 4 Ma (Phillips et al. 1997) and 1900-1700 Ma (Shee et al. 1999). The eastern part of the Yilgarn Craton includes older UML, carbonatites and kimberlites with an age of 2025 ± 10 Ma (Graham et al. 2004) and the late Archean CAL with ages of 2684 - 2640 Ma (Perring et al. 1989; McNaughton et al. 2005). Finally, UML at Norseman in

the southern margin of the craton occur with an age of 849 ± 9 Ma (Robey et al. 1989).

3 Results

3.1 Volatile elements (mineral chemistry)

Amphibole, mica and apatite are common minerals in alkaline rocks and can be used as an important indicator to reveal magma evolution. In the alkaline rocks of the Yilgarn Craton, amphibole is the dominant phenocryst phase in the CAL, whereas mica (phlogopite and tetraferriphlogopite) is the dominant phenocryst and macrocryst in UML, carbonatites, and orangeites. Apatite occurs as inclusions in amphibole phenocrysts of the CAL, as well as a groundmass phase in the other studied rock types.

Amphibole phenocrysts in the CAL contain F contents up to 0.6 wt.%, which is similar to or higher than magmatic amphibole from global lamprophyre occurrences (Tappe et al. 2004; Rock 1991). Phlogopite phenocrysts in the UML exhibit F contents (~ 1.5 wt.%), higher than those found in the global UML (Rock 1991; Tappe et al. 2004). The carbonatites contain both phlogopite and tetraferriphlogopite, displaying the highest F contents (~2.6 wt.%). Fluorine contents in tetraferriphlogopite grains from the orangeites are moderate (up to 0.5 wt.%). Overall, both amphibole and mica phenocrysts of the studied rocks are generally enriched in F.

Apatite grains in the studied CAL and carbonatites are enriched in F up to 5.1 wt.%, which is higher than average F contents in magmatic apatite from global silicate magma occurrences (Webster and Piccoli 2015). Fluorine contents in apatite from the UML and orangeites are similar or less than the average contents (~2.3 wt.%; Webster and Piccoli 2015). Sulfur contents in apatite from the examined CAL and one UML are enriched (~ 2 wt.%), which are much higher than average S concentrations found in global magmatic apatite occurrences from silicate and carbonate magmas (Belousova et al. 2002; Webster and Piccoli 2015).

3.2 Major, trace, volatile elements (whole-rock geochemistry)

Whole-rock data exhibit different geochemical characteristics for the different alkaline rock types. The CAL show distinct geochemistry and have higher SiO_2 and Na_2O (~ 60 and, 8 wt.%, respectively) with lower contents of K_2O (~ 3 wt.%), MgO (~ 12 wt.%) and TiO_2 (~ 1 wt.%) compared to the other alkaline rocks. They show significant primitive mantle-normalised negative Nb-Ta anomalies, whereas their CO_2 contents are highly variable (~ 11.6 wt.%), with relatively higher SO_3 contents (~ 0.5 wt.%) than the other rock types.

On the other hand, the UML, carbonatites, orangeites and kimberlites are generally characterised by low SiO_2 contents (< 42 wt.%) and high MgO, TiO_2 (~ 17 and 7 wt.% respectively) contents, similar to global UML (e..g, Tappe et al. 2008; Rock 1991) as well as orangeites (e.g., Mitchell 1995). In the primitive-mantle normalised patterns, the positive F anomalies are observed in these rocks. Their Ni and Cr contents are commonly high (up to ~1500, 2000 ppm).

3.3 PGE-Au (whole-rock geochemistry)

Primitive-mantle normalised PGE patterns of the CAL show strong fractionation with highly elevated $(Pd/Ir)_N$ ratios up to ~44. The CAL display highly variable Pt/Ir (up to ~ 58) with moderate Pt/Pd (mostly less than ~1.5) and Ru/Ir (~ 2.0) ratios. These features are also observed in the global CAL (Rock 1991; Gan and Huang 2017), however, the studied CAL contain higher Ir, Ru and Rh contents than the CAL from China (Gan and Huang 2017).

On the other hand, the UML, carbonatites, orangeites, and kimberlites are characterised by less fractionated PGE patterns, with $(Pd/Ir)_N$ ratios as low as ~11, which is similar to those found in kimberlites from South Africa and Finland (Maier et al. 2017). These rocks have similar Pd/Pt (~1.7) ratios to the CAL, whereas contain much lower Pt/Ir (~ 18) and higher Ru/Ir (up to ~2.8) ratios. In particular, the UML and carbonatites display lower Ir, Ru and Rh contents than other rock types, whereas the kimberlites and orangeites have higher Ir, Ru and Rh contents.

Interestingly, all the examined samples in this study exhibit primitive-mantle normalised positive Au-anomalies, with absolute values generally higher than the average contents of the primitive-mantle (McDonough and Sun 1995). These elevated Au contents are higher than any reported contents in kimberlites (Maier et al. 2017; McDonald et al. 1995).

4 Discussion

4.1 PGE distribution in the mantle

The alkaline rocks analysed in this study were most likely generated by small degrees of partial melting of the mantle and probably from different source depths. The variably fractionated but ubiquitously enriched PGE signature of all studied alkaline systems may reflect an inherited difference in the metallogenic endowment of the source, which would in turn point to the presence of spatially defined different pre-existing metasomatised domains in the mantle underlying the Yilgarn Craton.

4.2 Fluorine, sulfur and gold enrichment

The alkaline rocks from the Yilgarn Craton consistently display a strong positive Au anomaly in their primitive-mantle normalised patterns as well as higher Au contents than the primitive-mantle. These features are also observed in kimberlites and orangeites from Finland and South Africa (Maier et al. 2017; McDonald et al. 1995). This observation is potentially consistent with studies suggesting that spatially constrained metasomatised portions of the lithospheric mantle may be relatively enriched in Au (Maier et al. 2017; Tassara et al. 2018; Tassara et al. 2017).

In general, the key constituent magmatic minerals, such as amphibole, mica and apatite, of alkaline magmas from the Yilgarn Craton are anomalously enriched in F and S. It is argued that these volatiles may play a crucial role in the transport and concentration of precious metals from the mantle into the crust, and may go some way to explaining the metal endowment of the Yilgarn Craton.

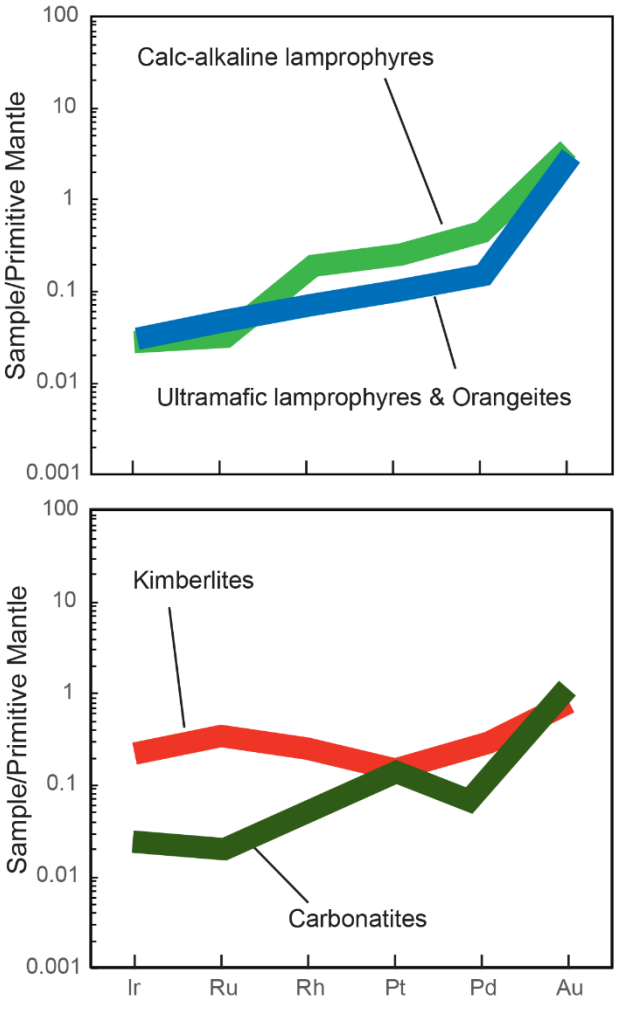

Figure 1. Primitive-mantle normalised PGE patterns of the various alkaline rock types in the Yilgarn Craton. Note that each line represents the average PGE contents of the different rock types: the bright green line (CAL; N = 21), blue line (UML and orangeites; N = 10), red line (kimberlites; N = 5), and dark green line (carbonatites; N=4).

Acknowledgements

This study is supported by the Australian Government through an Australian Government Research Training Program Scholarship and the Minerals Research Institute of Western Australia Postgraduate Scholarship, and by Australian Research Council Centre of Excellence for Core to Crust Fluid System.

References

Barley M, Brown S, Cas R, Cassidy K, Champion D, Gardoll S, Krapez B (2003) An integrated geological and metallogenic framework for the eastern Yilgarn Craton: developing geodynamic models of highly mineralised Archaean granite–greenstone terranes. AMIRA Project P 624.

Belousova E, Griffin W, O'Reilly SY, Fisher N (2002) Apatite as an indicator mineral for mineral exploration: trace-element compositions and their relationship to host rock type. Journal of Geochemical Exploration 76:45-69.

Blewett RS, Henson PA, Roy IG, Champion DC, Cassidy KF (2010) Scale-integrated architecture of a world-class gold mineral system: the Archaean eastern Yilgarn Craton, Western Australia. Precambrian Research 183:230-250.

Cassidy Kf, Champion DC, Krapez B, Barley ME, Brown SJA, Bleweet RS, Groenewald PB, Tyler IM (2006) A revised geological framework for the Yilgarn Craton, Western Australia. Geological Survey of Western Australia.

Czarnota K, Champion D, Goscombe B, Blewett R, Cassidy K, Henson P, Groenewald P (2010) Geodynamics of the eastern Yilgarn Craton. Precambrian Research 183:175-202.

Gan T, Huang Z (2017) Platinum-group element and Re-Os geochemistry of lamprophyres in the Zhenyuan gold deposit, Yunnan Province, China: Implications for petrogenesis and mantle evolution. Lithos.

Graham S, Lambert D, Shee S (2004) The petrogenesis of carbonatite, melnoite and kimberlite from the Eastern Goldfields Province, Yilgarn Craton. Lithos 76:519-533.

Griffin W, Begg G, O'reilly SY (2013) Continental-root control on the genesis of magmatic ore deposits. Nature Geoscience 6:905-910.

Griffin WL, Belousova EA, Shee SR, Pearson NJ, O'reilly SY (2004) Archean crustal evolution in the northern Yilgarn Craton: U–Pb and Hf-isotope evidence from detrital zircons. Precambrian Research 131:231-282.

Maier W, O'Brien H, Peltonen P, Barnes S-J (2017) Platinum-group element contents of Karelian kimberlites: Implications for the PGE budget of the sub-continental lithospheric mantle. Geochimica et Cosmochimica Acta 216:358-371.

McDonald I, De Wit M, Smith C, Bizzi L, Viljoen K (1995) The geochemistry of the platinum-group elements in Brazilian and southern African kimberlites. Geochimica et Cosmochimica Acta 59:2883-2903.

McDonough WF, Sun S-S (1995) The composition of the Earth. Chemical geology 120:223-253.

McNaughton NJ, Mueller AG, Groves DI (2005) The age of the giant Golden Mile deposit, Kalgoorlie, Western Australia: ion-microprobe zircon and monazite U-Pb geochronology of a synmineralization lamprophyre dike. Economic Geology 100:1427-1440.

Mitchell RH (1995) Kimberlites, orangeites, and related rocks. Springer Science & Business Media.

Mole DR, Fiorentini ML, Cassidy KF, Kirkland CL, Thebaud N, McCuaig TC, Doublier MP, Duuring P, Romano SS, Maas R, Belousova EA, Barnes SJ, Miller J (2013) Crustal evolution, intra-cratonic architecture and the metallogeny of an Archaean craton. Geological Society, London, Special Publications 393:23-80.

Mole DR, Fiorentini ML, Thebaud N, Cassidy KF, McCuaig TC, Kirkland CL, Romano SS, Doublier MP, Belousova EA, Barnes SJ, Miller J (2014) Archean komatiite volcanism controlled by the evolution of early continents. Proc Natl Acad Sci U S A 111:10083-10088.

Myers JS (1995) The generation and assembly of an Archaean supercontinent: evidence from the Yilgarn craton, Western Australia. Geological Society, London, Special Publications 95:143-154.

Pawley MJ, Wingate MTD, Kirkland CL, Wyche S, Hall CE, Romano SS, Doublier MP (2012) Adding pieces to the puzzle: episodic crustal growth and a new terrane in the northeast Yilgarn Craton, Western Australia. Australian Journal of Earth Sciences 59:603-623.

Perring CS, Rock NM, Golding SD, Roberts DE (1989) Criteria for the recognition of metamorphosed or altered lamprophyres: a case study from the Archaean of Kambalda, Western Australia.

Precambrian Research 43:215-237.
Phillips D, Fouriel F, Kiviets GB (1997) 40Ar/39Ar laser probe analyses of goundmass phlogopite grains from the Jewill kimberlite Yilgarn Craton, Western Australia. Anglo American Research Laboratories (unpublished).
Robey J, Bristow J, Marx M, Joyce J, Danchin R, Arnott F (1989) Alkaline ultrabasic dikes near Norseman, Western Australia. Kimberlites and Related Rocks 1:383-391.
Rock NMS (1991) Lamprophyres. Springer Science & Business Media.
Shee SR, Vercoe SC, Wyatt BA, Hwang PH, Campbell AN, Colgan EA (1999) Discovery and geology of the Nabberu kimberlite province, Western Australia Proceedings of the VIIth International Kimberlite Conference. pp 764-787.
Tappe S, Jenner GA, Foley SF, Heaman L, Besserer D, Kjarsgaard BA, Ryan B (2004) Torngat ultramafic lamprophyres and their relation to the North Atlantic Alkaline Province. Lithos 76:491-518.
Tappe S, Foley SF, Kjarsgaard BA, Romer RL, Heaman LM, Stracke A, Jenner GA (2008) Between carbonatite and lamproite—diamondiferous Torngat ultramafic lamprophyres formed by carbonate-fluxed melting of cratonic MARID-type metasomes. Geochimica et Cosmochimica Acta 72:3258-3286.
Tassara S, González-Jiménez JM, Reich M, Schilling ME, Morata D, Begg G, Saunders E, Griffin WL, O'Reilly SY, Grégoire M (2017) Plume-subduction interaction forms large auriferous provinces. Nature Communications 8.
Tassara S, González-Jiménez JM, Reich M, Saunders E, Luguet A, Morata D, Grégoire M, van Acken D, Schilling ME, Barra F (2018) Highly siderophile elements mobility in the subcontinental lithospheric mantle beneath southern Patagonia. Lithos 314:579-596.
Webster JD, Piccoli PM (2015) Magmatic apatite: A powerful, yet deceptive, mineral. Elements 11:177-182.
Wilde SA, Middleton MF, Evans BJ (1996) Terrane accretion in the southwestern Yilgarn Craton: evidence from a deep seismic crustal profile. Precambrian Research 78:179-196.

Widespread PGE depletion in the Tarim CFBs of NW China and implications for the ore potential in the Tarim LIP

Yin-Qi Li, Zi-Long Li, Shu-Feng Yang, Han-Lin Chen
Zhejiang University, China

Ya-Li Sun
Chinese Academy of Sciences

Abstract. The Early Permian Tarim Large Igneous Province (LIP) in northwestern China consists of voluminous continental flood basalts (CFBs) that can be classified into three groups. All of them exhibit extreme depletion in platinum group elements (PGE; ΣPGE < 1 ppb). Such widespread PGE depletion indicates that their parental magmas were likely to have been S-saturated before final eruption and/or there are residual S remaining in the mantle source during melting. The almost identical PGE depletion in both the more crustal contaminated and the least crustal contaminated basalts suggests that crustal contamination did not trigger the S saturation in the Tarim CFBs. Sulfur concentration at sulfide saturation estimation suggests that low-degree (ca. 5%) partial melting of the Tarim LIP's mantle source may play an important role on the widespread PGE depletion in the Tarim CFBs, residual S in the mantle takes most PGE from the basaltic magma. Furthermore, the evidence of magma mixing by magma chamber replenishment during the basalt eruptions in the Keping area supports secondary S-saturation for the basaltic magmas in the crust, which may cause PGE enrichment in some parts of the magma conduit. Therefore, it is still possible to discover the magmatic sulfide deposit in the Tarim LIP, which will probably be similar to the Voisey's Bay magmatic sulfide deposit in Canada.

1 Introduction

As one of the five Large Igneous Province (LIP) events occurred during Permian, the ca. 290 Ma Tarim LIP in the Tarim basin of northwest China comprises a diverse range of magmatic rocks from ultramafic–mafic to felsic compositions, and has been widely regarded as being genetically linked to a mantle plume (Li et al. 2012; Xu et al. 2014). Many LIPs around world possess world class Ni–Cu–PGE magmatic ore deposits, such as the Siberian Traps and Bushveld Complex. Although by far no Ni–Cu–PGE deposits are found in the Tarim LIP, a number of coeval Ni–Cu–(PGE) magmatic ore deposits have been reported around the Tarim Basin (Chai et al. 2008; Yang 2011). Whether the Tarim LIP has the potential of Ni–Cu–PGE magmatic ore deposits has also generated considerable interest among geologists leading to a number of recent investigations (e.g., Pirajno et al. 2009; Qin et al. 2011).

PGEs (Os, Ir, Ru, Rh, Pt and Pd) are highly siderophile elements that provide valuable information on the petrogenesis of mantle-derived igneous rocks. The PGE abundances in the CFBs are much lower as compared to lithophile elements, usually at ppb or even ppt level. Nevertheless, they are potential markers of the magmatic process and source nature of the basalts. They are particularly sensitive for the extent of sulfur saturation and sulfide segregation (Barnes et al. 1985; Keays 1995). In addition, variations in the concentrations and ratios between different PGE can provide important information relating to the genesis of magmatic Ni–Cu–PGE sulfide mineralization. A number of studies have proposed that the giant Noril'sk–Talnakh Ni–Cu–PGE sulfide ore is associated with the PGE-depleted basalts of the Nadezhdinsky Formation in the Siberian Traps (Naldrett et al. 1992).

In this study, PGE geochemistry of the Tarim continental flood basalts (CFBs) are systematically studied to address the sulfur saturation and evolution process of the Tarim CFB magmas and evaluate the Cu–Ni–PGE mineralization potential of the TLIP.

2 Geological background

The Tarim Basin in the northwest China, surrounded by the Tianshan, Kunlun and Altyn–Tagh orogenic belts, mainly consists of Precambrian crystalline basement and Phanerozoic strata from the Ordovician to Neogene. Some important tectonothermal activities from the Archean to Paleozoic have been identified in this area, in which the early Permian magmatic event (known as the Tarim LIP) was regarded as the most important one. The Tarim LIP is widely distributed in the Tarim Basin. Large scale continental flood basalt lavas were erupted during the Early Permian, constituting the main part of the Tarim LIP. Systematic geochronological studies have concluded that the main eruptions of the Tarim CFBs occurred in a period of ~5 Myr close to 290 Ma (Li et al. 2011). A diverse assemblage of coeval intrusive rocks, such as layered mafic–ultramafic intrusions, mica–olivine pyroxenite breccia pipes, diabase and ultramafic dykes, quartz syenites, diorite, quartz syenite porphyry and bimodal dykes, were also emplaced in the Tarim Basin (Li et al. 2012).

The Tarim CFBs are mostly high-Ti basalts (TiO_2 > 2.5 wt.% and Ti/Y > 500) belonging to the alkaline series. In general, they exhibit significant enrichments of large-ion lithophile and light rare-earth elements on the primitive mantle-normalized spidergram, which are similar to the ocean island basalts (OIBs) except the slight Nb–Ta depletion (Fig. 1). Their high Ti/Y and Zr/Y ratios support

a within-plate petrogenetic affinity.

Based on their geochemical distinctions, the Tarim CFBs can be subdivided into three. Groups 1a and 1b basalts are widely distributed within the Tarim Basin. They have many similar petrological and geochemical characteristics, but the earlier erupted Group 1b basalts show higher Th/Nb ratios (mostly >0.2), and exhibit fairly low Nb/U (<21) and Ce/Pb (<12) ratios, indicating more crustal contamination than the latter group 1a basalts (Li et al. 2014). Conversely, Group 2 basalts so far are only identified from four drill holes in the Northern Tarim Basin. They show a clear depletion on the heavy rare-earth elements, have higher Nb/Yb ratios (≥15) that approach those of OIB. These geochemical features indicate that Group 2 basalts are less crustally contaminated and more similar to OIB in composition than both Groups 1a and 1b basalts. Differences among the three group basalts can also be discerned from their distinctive Sr and Nd isotopic characteristics, suggesting heterogeneous source compositions and variable crustal contamination during the generation of the Tarim CFBs.

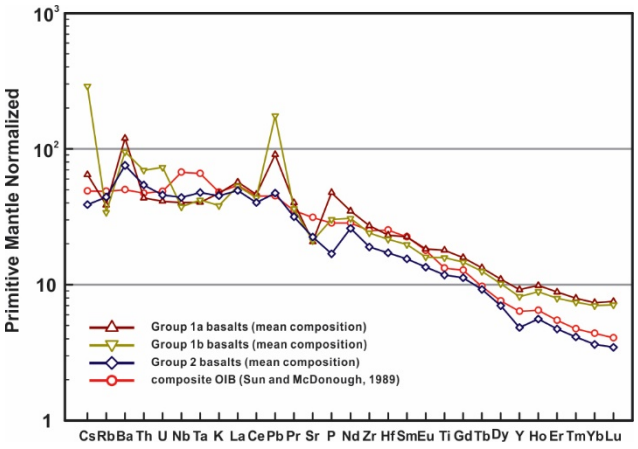

Figure 1. Primitive mantle normalized element abundance patterns for the three group basalts in the Tarim LIP.

3 PGE geochemistry of the Tarim CFBs

Twenty-five basalt samples from different locations in the Tarim LIP were selected to analyze their PGE contents. Among them, 19 samples are Group 1a basalts from the Northern, Southwestern and Central Tarim Basin; 2 samples are Group 1b basalts from the Northern Tarim Basin; and 4 samples are Group 2 basalts from the drill holes in the Northern Tarim Basin.

All the three group basalts from different locations in the TLIP exhibit extremely low PGE contents (Os 0.001–0.106 ppb, Ir 0.000–0.067 ppb, Ru 0.004–0.253 ppb, Rh 0.001–0.078 ppb, Pt 0.031–0.376 ppb, Pd 0.026–0.168 ppb and ∑PGEs = 0.078–0.723 ppb; Table 1). Apart from PGE, the Tarim CFBs also display low Cu contents (mostly < 100 ppm). On the primitive mantle normalized plot, basalts from the same section (or the same location) display similar PGE pattern. Except those from the Keping area (12 Group 1a basalts and 2 Group 1b basalts), they generally show an enriched trend from Os to Pd in Pt and Pd than the other PGEs, similar to other CFBs around the world (Barnes et al. 1985).

Table 1. PGE and Cu concentrations of basalts from the TLIP, Siberian Traps, ELIP, East Greenland CFBs and Deccan Traps.

	N	Ir (ppb)	Pd (ppb)	Cu (ppm)	Pd/Ir	Cu/Pd ($\times10^5$)
Tarim LIP	36	0–0.067	0.015–0.275	24.7–223	0.34–39.9	1.55–32.9
Siberian Traps (Nadezhdinsky Formation)	15	<0.01	0.07–0.46	20–89	–	0.89–8.86
Siberian Traps (except Nadezhdinsky Formation)	39	0.03–1.68	1.42–17.4	44–498	4.40–276	0.09–0.44
ELIP (high Ti basalts)	115	0.009–0.88	0.3–32.6	28.5–292	6.11–850	0.03–1.60
Deccan	31	0.05–0.49	2.35–31.8	105–347	12.6–330	0.08–0.68
East Greenland	35	0.05–1.58	3.04–25	43–453	2.07–346	0.09–0.35

Note: N is the number of samples. The Tarim LIP basalts data are from this study and Yuan et al. (2012), the Siberian Traps basalts data are from Lightfoot and Keays (2005), the ELIP high-Ti basalts data area from Qi et al. (2008) and Song et al. (2009), and the East Greenland basalts data are from Momme et al. (2002).

4 Discussion

4.1 S-saturated Tarim CFB magmas

Compared with other CFBs around the world, the PGE concentrations (represented by Ir and Pd) in the Tarim CFBs appear to be strongly depleted, only similar to those PGE-depleted basalts in the Nadezhdinsky Formation in the Siberian Traps (Table 1). PGEs are generally partitioned into immiscible sulfide liquids during sulfide segregation due to their extremely high sulfide liquid/silicate melt partition coefficients (Fleet et al. 1991), causing their concentrations to decrease in the residual silicate magma. Cu, Pd and Ir are often used to judge the magma's sulfur saturation state. Pd and Ir show compatible behavior in sulfide phase when a suite of lavas undergoes S-saturated differentiation, due to their sulfide liquid/silicate melt partition coefficients ($D^{Sul/Sil}$) being of the order of 10^3 to 10^5 (Song et al. 2009). The $D^{Sul/Sil}$ of Cu (10^2 to 10^3) is much lower than the PGEs, which indicates that the Cu/Pd ratio will strongly increase once sulfide liquids segregate from the silicate magma (Campbell and Barnes 1984). In contrast, both Cu and Pd behave as incompatible elements in S-undersaturated systems, but the Pd/Ir ratio increases during S-undersaturated differentiation (Momme et al. 2002). This is because Pd is an incompatible element whereas Ir behaves as a compatible element during silicate fractionation of a basaltic magma (Keays 1995).

The Tarim CFBs have extremely high Cu/Pd ratios (>10^5) with a narrow range of lower Pd/Ir ratios (<50),

which can be easily distinguished from the S-undersaturated and PGE-undepleted basaltic suites from the Siberian Traps, ELIP, East Greenland CFB and Deccan Traps (Fig. 2a). Besides, the Tarim CFBs also exhibit generally lower Cu/Zr ratios than the PGE-depleted PGE-depleted basalts in the Nadezhdinsky Formation in the Noril'sk region in the Siberian Traps (Fig. 2b), reflecting Cu depletion (Keays and Lightfoot 2010). These features, combined with the extremely low PGE and Cu contents, suggest that the parental magmas of the Tarim CFBs have been S-saturated before final eruption.

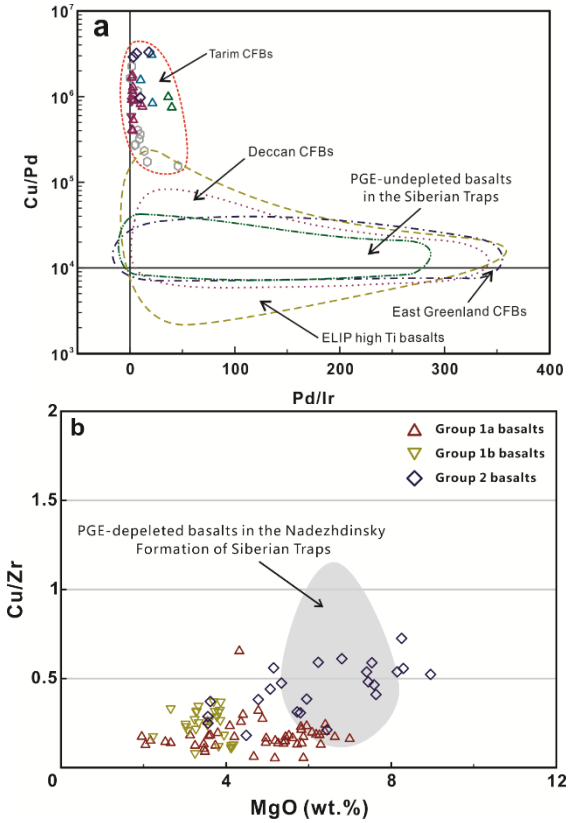

Figure 2. (a) Scattergram of Pd/Ir vs. Cu/Pd showing the fields of the Tarim CFB, PGE-undepleted basalts in the Siberian Traps, ELIP, East Greenland and Deccan. (b) Scattergram of MgO vs. Cu/Zr showing the distributions of the three group basalts in the TLIP. Data sources are the same as for Table 1.

4.2 Possible reason for S-saturation in the Tarim CFB magmas

Crustal contamination is commonly considered as the main reason to cause S-saturation in mantle-derived magmas (Keays and Lightfoot 2010). The Tarim CFBs in different locations have suffered variable degrees of crustal contamination, whereas both more contaminated Group 1 basalts and less contaminated Group 2 basalts show strong depletion in PGE. Therefore, crustal contamination during the Tarim basalt eruptions may not trigger S-saturation in their parental magmas. The S-saturation process are more likely to be related to the magma source region.

Although the Tarim CFBs in different locations may have variable source compositions, calculations based on trace element geochemistry from the Tarim CFB suggest that their parent magmas were derived from <5% partial melting of the mantle source (Yu et al. 2011; Zhou et al. 2009), consistent with their alkaline nature and LILE- and LREE-enriched trace element signature. The S content of the mantle reservoir is generally about 150–250 ppm, and therefore melts derived by ca. 5% partial melting would contain 3000 to 5000 ppm S from a columnar melting regime (Keays 1995). Whereas the estimated sulfur concentration at sulfide saturation (SCSS) for the Tarim CFB magmas range from 859 to 1929 ppm, which is much lower than the S content produced by their partial melts. In this scenario, a substantial amount of residual sulfide would be left behind in the mantle, and only a small portion of the PGEs would be released to the silicate partial melts, which may account for the significant PGE depletion of all the Tarim CFBs. The fact that all the known Tarim CFBs in the TLIP are exclusively PGE-depleted also indicates that their parent magmas have been S-saturated at the same stage, probably when they emerged from the mantle.

Furthermore, Fig. 3 shows that there is a negative correlation between the PGE concentrations and εNd(t) values for the basalt sequence in the Keping area, indicating that a continuously influx of relatively primitive and uncontaminated magma of the same lineage into a chamber occupied by evolved residual magma. Mixing of an evolved magma with appropriate amounts of a primitive magma is capable of achieving sulfur saturation in the hybrid (Li et al. 2001), which may trigger a certain extent of sulfide segregation and PGE depletion in the basalt sequence, although the feature is not so prominent due to their extremely low PGE contents. Such a magma chamber replenishing process is also supported by the general decreasing trend of the $(La/Yb)_N$ ratios from the base to the top basaltic units in the Yingan section, which eventually led to multiple basaltic flows in the Keping area (Yu et al. 2011).

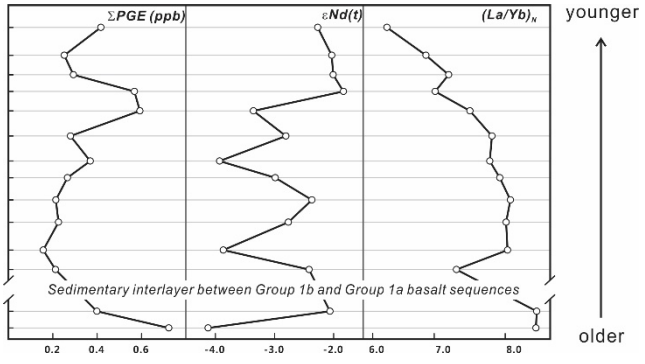

Figure 3. PGE, εNd(t) and $(La/Yb)_N$ systematic variations for the basalt sequences in the Keping area.

5 Implications for the Cu–Ni–PGE mineral resource potential in the TLIP

The above considerations indicate that the degree of partial melting plays an important role on the Cu–Ni–PGE mineralization in the TLIP. Due to very low degrees of

partial melting, the Tarim CFBs are extremely PGE-depleted, which may account for the absence of Cu–Ni–PGE sulfide deposit in the TLIP. Mafic–ultramafic rocks formed by high-degree partial melting from the mantle source in the TLIP should receive more attention in terms of their Cu–Ni–PGE mineralization potential. In fact, a number of similar deposits are reported in the Eastern Tianshan and Beishan area, and recent studies suggest that they may also be a part of the TLIP (Pirajno et al. 2009; Qin et al. 2011). It is also noted that the PGE geochemistry of basalts in the Yingan section indicates that magma replenishment in the magma chamber may trigger s-saturation in the evolved magma. The latter may cause the magma become S-saturated again and segregate the saturated sulfide in the crust before final eruptions (Naldrett 2004), which may be possible to develop a Cu–Ni–PGE sulfide deposit in the Tarim LIP.

Acknowledgements

This study was jointly funded by the National Natural Science Foundation of China (41603029 and 40930315) and the National Basic Research Program of China (973 Program: 2011CB808902 and 2007CB411303).

References

Barnes S-J, Naldrett AJ, Gorton MP (1985) The origin of the fractionation of platinum-group elements in terrestrial magmas. Cheml Geol 53: 303–323.

Campbell IH, Barnes SJ (1984) A model for the geochemistry of the platinum-group elements in magmatic sulfide deposits. Can Mineral 22: 151–160.

Chai F, Zhang Z, Mao J, Dong L, Zhang Z, Wu H (2008) Geology, petrology and geochemistry of the Baishiquan Ni–Cu-bearing mafic–ultramafic intrusions in Xinjiang, NW China: Implications for tectonics and genesis of ores. J Asian Earth Sci 32: 218–235.

Fleet ME, Tronnes RG, Stone WE (1991) Partitioning of platinum group elements in the Fe–O–S system to 11 GPa and their fractionation in the mantle and meteorites. J Geophys Res 96: 21949–21958.

Keays RR (1995) The role of komatiitic and picritic magmatism and S-saturation in the formation of ore deposits. Lithos 34: 1–18.

Keays RR, Lightfoot PC (2010) Crustal sulfur is required to form magmatic Ni–Cu sulfide deposits: evidence from chalcophile element signatures of Siberian and Deccan Trap basalts. Miner Deposita 45: 241–257.

Li C-S, Maier WD, De Waal SA (2001) The role of magma mixing in the genesis of PGE mineralization in the Bushveld Complex: Thermodynamic calculations and new interpretations. Econ Geol 96: 653–662.

Li Y, Li Z, Yu X, Langmuir CH, Santosh M, Yang S, Chen H, Tang Z, Song B, Zou S (2014) Origin of the Early Permian zircons in Keping basalts and magma evolution of the Tarim Large Igneous Province (northwestern China). Lithos 204: 47–58.

Li Z, Chen H, Song B, Li Y, Yang S, Yu, X (2011) Temporal evolution of the Permian large igneous province in Tarim Basin in northwestern China. J Asian Earth Sci 42: 917–927.

Li Z, Li Y, Chen H, Santosh M, Yang S, Xu Y, Langmuir CH, Chen Z, Yu X, Zou S (2012) Hf isotopic characteristics of the Tarim Permian large igneous province rocks of NW China: Implication for the magmatic source and evolution. J Asian Earth Sci 49: 191–202.

Lightfoot PC, Keays RR (2005) Siderophile and chalcophile metal variations in flood basalts from the Siberian Trap, Noril'sk Region: Implications for the origin of the Ni–Cu–PGE sulfide ores. Econ Geol 100: 439–462.

Momme P, Tegner C, Brooks CK, Keays RR (2002) The behaviour of platinum-group elements in basalts from the East Greenland rifted margin. Contrib Mineral Petrol 143: 133–153.

Naldrett AJ (2004) Magmatic Sulfide Deposits: Geology, Geochemistry and Exploration. Springer, Berlin: 728 pp.

Naldrett AJ, Lightfoot PC, Fedorenko VA, Doherty W, Gorbachev NS (1992) Geology and geochemistry of intrusions and flood basalts of the Noril'sk region, USSR, with implications for the origin of the Ni–Cu ores. Econ Geol 87: 975–1004.

Pirajno F, Ernst RE, Borisenko AS, Fedoseev G, Naumov EA (2009) Intraplate magmatism in Central Asia and China and associated metallogeny. Ore Geol Rev 35: 114–136.

Qi L, Wang CY, Zhou M-F (2008) Controls on the PGE distribution of Permian Emeishan alkaline and peralkaline volcanic rocks in Longzhoushan, Sichuan Province, SW China. Lithos 106: 222–236.

Qin K, Su B, Sakyi PA, Tang D, Li X, Sun H, Xiao Q, Liu P (2011) SIMS zircon U–Pb geochronology and Sr–Nd isotopes of Ni–Cu-bearing mafic–ultramafic intrusions in Eastern Tianshan and Beishan in correlation with flood basalts in Tarim Basin (NW China): Constraints on a ca. 280 Ma mantle plume. Am J Sci 311: 237–260.

Song X, Keays RR, Xiao L, Qi H, Ihlenfeld C (2009) Platinum-group element geochemistry of the continental flood basalts in the central Emeishan Large Igneous Province, SW China. Chem Geol 262: 246–261.

Sun S-S, McDonough WF (1989) Chemical and isotopic systematics of oceanic basalts: implications for mantle composition and processes, in: Saunders AD, Norry MJ (Eds.), Magmatism in the Ocean Basins. Geol Soc, London, Spec Pub 42: 313–345.

Xu Y, Wei X, Luo Z, Liu H, Cao, J (2014) The Early Permian Tarim Large Igneous Province: Main characteristics and a plume incubation model. Lithos 204: 20–35.

Yang S, (2011) The Permian Pobei Mafic–Ultramafic Intrusion (NE Tarim, NW China) and Associated Sulfide Mineralization. Ph.D. Thesis, The University of Hong Kong, 261 pp.

Yu X, Yang S, Chen H, Chen Z, Li Z, Batt GE, Li YQ (2011). Permian flood basalts from the Tarim Basin, Northwest China: SHRIMP zircon U–Pb dating and geochemical characteristics. Gondwana Res 20: 485–497.

Yuan F, Zhou T, Zhang D, Jowitt SM, Keays RR, Liu S, Fan Y, 2012. Siderophile and chalcophile metal variations in basalts: Implications for the sulfide saturation history and Ni–Cu–PGE mineralization potential of the Tarim continental flood basalt province, Xinjiang Province, China. Ore Geol Rev 45: 5–15.

Zhou M-F, Zhao J, Jiang C, Gao J, Wang W, Yang S (2009) OIB-like, heterogeneous mantle sources of Permian basaltic magmatism in the western Tarim Basin, NW China: Implications for a possible Permian large igneous province. Lithos 113: 583–594

Using Platinum Group Element geochemistry to determine magma fertility of Mount Hagen, Papua-New Guinea

Monika Misztela, Ian Campbell
Research School of Earth Sciences, Australian National University, Canberra, Australia

Abstract. Mount Hagen is a Mid-Pleistocene stratovolcano located in Papua-New Guinea Highlands. The tectonic setting of the volcano has been a matter of considerable debate, with its complexity leading to different conclusions regarding magma source and classification. Two key questions remain unanswered: (i) is this "arc-like" magma related to a subduction zone and therefore part of an arc system? and, (ii) can it be related to potential porphyry style economic mineralisation?

Occurrence of porphyry deposits is strongly related to subduction zones, so the identification of tectonic setting is important for mineral exploration. If Mount Hagen is part of an arc system, is it barren or ore-bearing?

Assuming that sulfide saturation, relative to volatile saturation, is one of the main factors controlling magma fertility, PGE, Re and Au concentrations were measured by fire-assay isotope dilution method in 18 samples, to determine its potential to form an Au-Cu deposit. PGE were chosen to investigate the timing of S saturation because of their low solution mobility in hydrothermal fluids and their high partition coefficient into sulfide melts. Analyses showed that S saturation occurred early in the system (at 8 MgO wt%), which make it unlikely that the system will produce an Au-Cu deposit.

1 Background

Porphyry deposits are large, low grade, epigenetic, intrusion-related deposits that form in magmatic arcs above subduction zones in both oceanic and continental margins (Wilkinson 2013). These systems are the primary resource world`s Cu (nearly three-quarters) and Au (almost a half) (Sillitoe 2010). Even though their metal grades are low, their economic significance is compensated by their size, which makes them desirable for exploration companies.

Most of these systems occur in recent or old subduction zones, so the prospectivity is strongly determined by this factor. Every year, exploration companies invest millions of dollars in discovery of locations of new porphyry systems. The process of identification whether they are barren, or ore-bearing is time- and funds-consuming. Intrusion shape, the mineral phases and even the alteration haloes around both types can be the same, which makes the prospecting problematic. Money and time could be saved, if barren systems could be distinguished from ore-bearing ones at an early stage of exploration.

The starting hypothesis for this study is that the timing of sulfide saturation, relative to volatile saturation, plays a key role in porphyry system fertility. If S saturation starts early, all of the chalcophile elements, including Cu and Au, are trapped in sulfide phases in a deep magma chamber, and are unable to enter a fluid phase. The result is a barren system. However, if the S saturation occurs late, after or shortly before the volatile saturation, metals will be able to enter the fluid phase and form a deposit (Park 2012). To precisely identify timing of sulfide saturation in the samples, platinum group elements (PGE) concentrations were measured in rocks of varying MgO content, assuming that they are related by fractional crystallization. PGE were chosen because their partition coefficients into sulfides are higher than Cu (1000 times higher) and Au (100 times higher), which makes them very sensitive indicators of the S saturation. Furthermore, their solubility in hydrothermal fluids is 1000 to 100 times less than Cu and Au, so they are more reliable indicators of magmatic processes. PGE occur in rocks in very low concentration, so it is necessary to apply a suitable method that can measure these elements with the required precision. Recent advances in the NiS fire assay-isotope dilution method make it possible to detect the PGE at ultra-low levels (ppt) and apply it to rock suites associated with porphyry Cu deposits (Park 2012).

A known quantity of spike (a solution with a known, unnatural isotope composition) is added to a sample to determine the concentration of an element. It can be calculated by measuring spike-sample mixture at the end of the process by using the formula (Stracke et al. 2014):

$$A_{mix} = A_{sa} + A_{sp}$$
$$B_{mix} = B_{sa} + B_{sp}$$

(Where: A_{mix} – a mixture of a sample A_{sa} and spike A_{sp}; B_{mix} – a mixture of a sample B_{sa} and spike B_{sp})

2 Geological setting

Mount Hagen is a Pleistocene stratovolcano located in Western Highlands and Enga Provinces in Papua New Guinea (Mackenzie and Johnson 1984). It is the second highest volcano on both the island and on the Australian continent (3,778 m) and was formed during a magmatic period around 230,000 years ago. It is considered extinct with the last eruption taking place around 50,000 years ago (Mackenzie and Johnson 1984). The mountain lies on a folded Mesozoic and Cenozoic sedimentary sequence, which overlies late Palaeozoic granitic and metamorphic basement (Mackenzie 1972).

For many years, the tectonic setting of this very complex area of Papua New Guinea, and the formation of the Mount Hagen volcano were topics of discussion. Mackenzie (1972 and 1980) classified the volcano as belonging to an arc-like system, with no evidence for Benioff zone but with many geochemical similarities to arc systems. As most of the theories about formation of

porphyry deposits involve arc magmas, which are strongly associated with active subduction zones, there was no tectonic evidence to support the hypothesis that Mount Hagen could be related.

New theories suggest that porphyry deposits form even after tectonic activity on subduction zones stops (Richards 2009). Most likely, these magmas are products of remelting a previously subducted slab, activated during the post-subduction processes. Magmas formed this way normally do not host large amounts of sulfides. Recently, a number of porphyries have been related to magmas that were not associated with any contemporaneous subductions, however they are overlapping with the post-subduction processes or collisions between plates. This type of event is, in many ways, similar to subduction related calc-alkaline magmatism.

Recent reconstructions of Papua New Guinea microplate tectonics show that at around 4 Ma ago convergence between New Guinea and South Bismarck microplate led to a collision between Australian plate and an early Tertiary island-arc that later caused anticlockwise rotation of the New Britain arc (Hill and Hall 2003; Holm and Richards 2013; Koulali et al. 2015). This event eventually led to a subduction of Solomon Plate from northern and southern sides, creating a U-shape slab (Pegler 1995). This movement resulted in orogenesis, that is continuing to today, and formation of the New Guinea Mobile Belt. This, in turn, led to a series of thrusting and faulting at the continental margin (Jaques et al, 1977). Building on this hypothesis, Pegler (1995) suggested that the Solomon Plate`s southern slab is no longer active, and instead it is sinking under its own gravitational forces. Further uplift of Highlands triggered magmatic activity and formation of Mount Hagen from a subducted previously, partially melted slab (Jaques at al. 1977).

3 Samples and analytical methods

Forty-five whole-rock samples from Mount Hagen, which had previously been analysed for major elements by Mackenzie (1980), were obtained from the Australian National University and the University of Melbourne rock collections. Eighteen samples with a range of 2.04 to 11.5 MgO wt% were selected for further analysis.

The trace-element concentrations of all samples were measured by LA-ICP-MS at Research School of Earth Sciences at the Australian National University. Glass discs used for the analysis were prepared by mixing 0.5 g of rock powder and 1.5 g of flux (consists of 65% of lithium metaborate and 35% lithium tetraborate), and fused in an induction furnace. Calcium was used as an internal standard for the data reduction, NIST 610 as the primary standard, and NIST 612 and BCR-2G for quality control.

PGE, Re and Au concentrations were determined by the Ni-sulfide fire assay-isotope dilution method, described in detail by Park et al. (2012). Concentrations of these elements were measured by ICP-MS in solution mode at RSES. Selected samples were analysed in duplicate to monitor heterogeneity. To test the accuracy of the method, the standard TDB-1 was run during each analysis.

Chemical analyses of mineral phases were obtained by LA-ICP-MS at RSES and JEOL 8530F Plus Electron Probe Microanalyser at Centre for Advanced Microscopy (CAM), ANU. Eleven element and mineral distribution maps were also obtained by FEI Quanta QEMSCAN at CAM, ANU, using a step size of 15µm.

4 Results

4.1 Petrography and mineral composition

All the samples collected from Mount Hagen are moderately to strongly porphyritic, with phenocrysts of augite, olivine (samples with high MgO wt%) and hornblende (rocks with low MgO wt%) up to 4 mm, smaller plagioclase (1-2 mm), rarely biotite and microphenocrysts of Fe-Ti oxides. The groundmass in general consists of plagioclase (increasing with decreasing MgO content), alkali feldspar (decreasing with decreasing MgO content), ortho- and clinopyroxene, fine-grained Fe-Ti oxides, hornblende and apatite (Fig. 1).

Most of the plagioclase and pyroxene phenocrysts show oscillatory zoning. Plagioclases tend to have slightly more calcic cores and sodic rims. In general, pyroxenes show enrichment in Mg with slightly more calcic cores whereas olivines show enrichment in Mg in the cores and Fe in the rims. Often, olivine phenocrysts with diopside or ferrosillite rims can be observed in high-MgO samples.

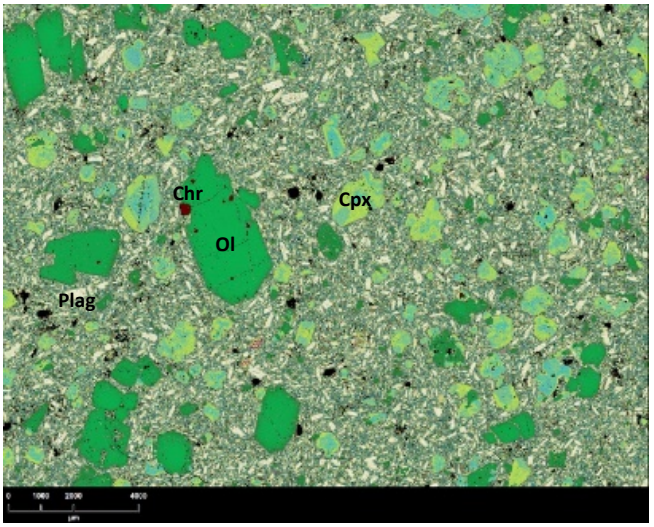

Figure 1. QEMSCAN image of 1707 thin section (11.5 MgO wt%). Cpx = here augite; Ol = forsterite; Plag = anorthite, Chr = chromite.

Most of the sulfides found in thin sections and polished mounts occur as rounded inclusions in pyroxenes of 5 to 20 µm in diameter (Fig. 2). Microprobe analysis of 6 of them show that they consist of 55 to 57 Fe wt.%, 38 S wt.%, 2.5 to 4 Ni wt.% in high MgO samples (referred as pyrrhotites $Fe_{6.7}Ni_{0.3-0.4}S_8$) and 33 to 41 Fe wt.%, 34 S wt.%, 17 to 29 Cu wt.% and up to 5.5 Ni wt% in low MgO ones (referred as chalcopyrites $Cu_{0.5-0.9}Fe_{1.1-1.4}Ni_{0-0.2}S_2$).

Figure 2. Rock thin section in optical microscope with reflected light.

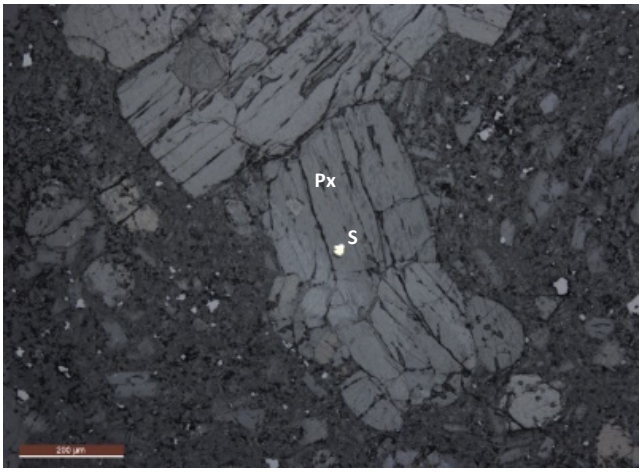

S = sulfide; Px = pyroxene.

4.2 Major- and trace-element geochemistry

Based on the alkali and silica content in samples, most of them were classified as basalts or andesites and form part of a calc-alkaline to high-K calc-alkaline series, typical of magmas from island arcs. (Fig.3).

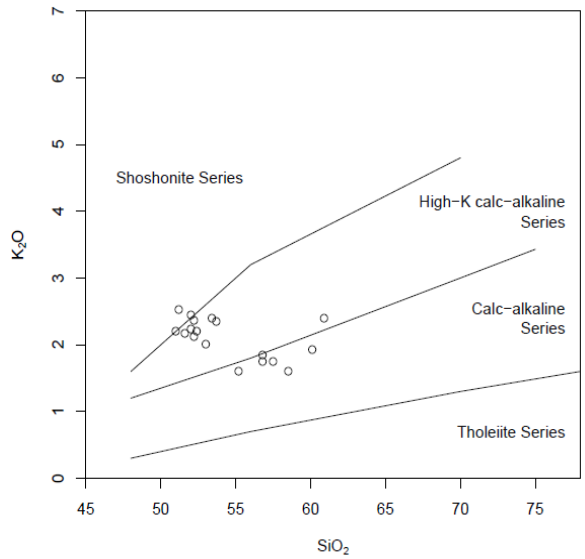

Figure 3. Classification diagram of K_2O vs SiO_2 (wt%) for the Mount Hagen samples.

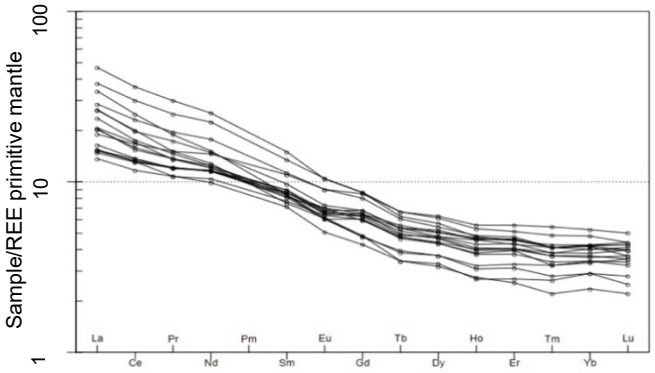

Figure 4. Primitive mantle-normalized whole rock rare earth element patterns for Mount Hagen samples.

Most of the primitive mantle-normalized rare earth element (REE) patterns of 18 samples are parallel to each other, suggesting that they come from the same system and are related by fractional crystallisation (Fig. 4).

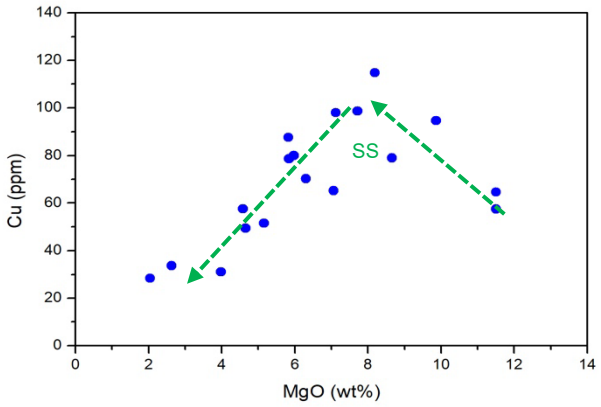

Figure 5. Variation of Cu vs MgO for samples from Mount Hagen suite. SS show the point of sulfide saturation

Plots of Cu (Fig. 5), Sc and V, together with total Fe as Fe_2O_3 (Fig. 6) and TiO_2 show that sulfide saturation coincides with the onset of magnetite crystallization (the magnetite crisis) and occurred at about 8 MgO wt%. This conclusion is consistent with the previous studies reporting that the crystallisation of magnetite often triggers sulfide saturation in the system (Jenner et al. 2012).

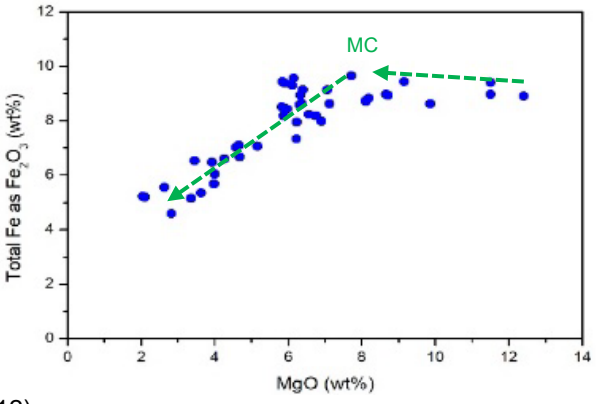

Figure 6. Variation of total Fe as Fe_2O_3 vs MgO for samples from Mount Hagen suite. MC show the magnetite crisis.

4.3 PGE and Re geochemistry

Disagreement between duplicate analyses for both Pt and Pd indicate the presence of nuggets before and after sulfide saturation (Fig. 7). In this case, disagreement after 8 MgO wt% was expected, as it had been seen in previous studies (Park 2012; Hao et al. 2017), but finding it in pre-sulfide saturation samples was a surprise. It is suggested that this nugget effect is due to the presence of sulfide inclusions in phenocrysts carried into the sulfide unsaturated magma. These were seen as sulfide inclusions in pyroxene phenocrysts during microprobe analysis of thin sections of high MgO samples (Fig. 2). It is suggested that sulfide saturation occurred in two

stages. The first took place at early phase of magma evolution, probably in the magma chamber at the crustal level, where the fractionation occurred (>12 MgO wt%) and pyroxene phenocrysts grew. It involved precipitation of a small amount of sulfide, which affected the PGE due to their high partition coefficient into sulfides but did not affect Cu. The second stage of sulfide saturation occurred later in the magma evolution process, at around 8 MgO wt%, this time affecting all the chalcophile elements, including Cu.

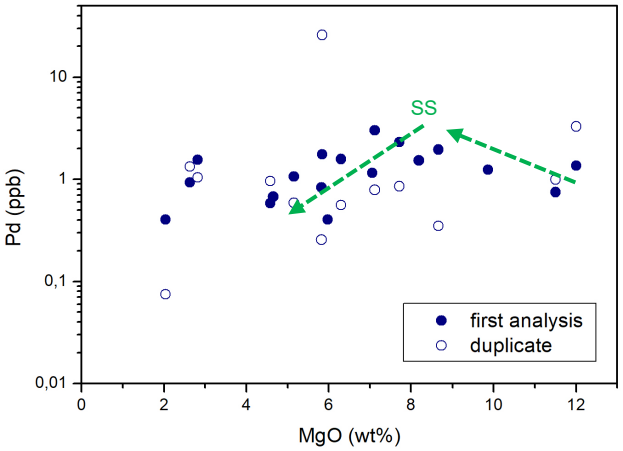

Figure 7. Plot of Pt vs MgO for samples from Mount Hagen suite. Green arrows show variations in Pd. SS show the point of sulfide saturation. Blue circles are results of the first analysis, empty ones of duplicates.

5 Conclusions and implications for the ore-forming process

Recent studies of Papua New Guinea microplate tectonics, together with geochemical data suggest that Mount Hagen magma resulted of post-collision remelting of a previously subducted slab. As a consequence, the Mount Hagen suite could potentially be related to a porphyry system.

Major- and minor elements imply that fractional crystallization was the main factor controlling the geochemistry of the studied suite. Some scattering is attributed to presence of phenocrysts and minor alterations.

The PGE in Mount Hagen volcanics show that S saturation occurred early in the system, which agrees with previous studies, suggesting that metals such as Cu and Au were trapped in the crystallizing magma chamber and were unable to enter a fluid phase (Hao, 2017). As a consequence, the residual magma would be depleted in these elements the suite unlikely to produce a Cu or Au deposit despite the favourable tectonic setting.

Acknowledgements

This work was supported by an ARC Discovery Project to Ian Campbell. We would like to thank prof. Richard Arculus and prof. Jon Woodhead for providing samples used in this study. The authors acknowledge the facilities, and the scientific and technical assistance, of Microscopy Australia at the Centre for Advanced Microscopy, The Australian National University.

References

Hill KC, Hall R (2003) Mesozoic-Cainozoic Evolution of Australia`s New Guinea Margin in a West Pacific Contex. Geological Society of Australia Special Publication, 22:265-290

Holm RJ, Richards SW (2013) A re-evaluation of arc-continent collision and along-arc variation in the Bismarc Sea region, Papua New Guinea. Australian Journal of Earth Sciences, 60:605-619

Hao H, Campbell IH, Park J-W, Cooke DR (2017) Platinum-group element geochemistry used to determine Cu and Au fertility in the Northparkes igneous suites, New South Wales, Australia. Geochimica et Cosmochimica Acta, 216:372-392

Jaques AL, Robinson GP (1977) The continent/island-arc collision in northern Papua New Guinea. BMR Journal of Australian Geology & Geophysics, 2:289-303

Koulali W, Tregoning P, McClusky S, Stanaway R, Wallace L, Lister G (2015) New insights into the present-day kinematic of the central and western Papua New Guinea from GPS. Geophysical Journal International, 202:993-1004

Mackenzie DE (1980) Volcanoes of the Papua New Guinea Highlands: volcanism on a continental margin and its relationship to subduction. Dissertation, University of Melbourne

Mackenzie DE, Johnson RW (1984) Pleistocene volcanoes of the Western Paua New Guinea Highlands: morphology, geology, petrography and modal and chemical analysis. Bureau of Mineral Resources, Geology and Geophysics by the Australian Government Publishing Service

Park J-W (2012) Platinum-group element geochemistry of felsic rocks. Dissertation, Australian National University

Pegler G, Das S, Woodhouse JH (1995) A seismological study of the eastern New Guinea and the western Solomon Sea regions and its tectonic implications. Geophysical Journal International, 122:961-981

Stracke A, Scherer EE, Reynolds BC (2014) Application of Isotope Dilution in Geochemistry. Elsevier Ltd., 71-86

Richards JP (2009) Postsubduction porphyry Cu-Au and epithermal Au deposits: Products of remelting of subduction-modified lithosphere. Geology, 37:3:247-250

Silitoe RH (2010) Porphyry copper systems. Economic Geology, 105:3-41

Wilkinson JJ (2013) Triggers for the formation of porphyry ore deposits in magmatic arcs. Nature Geoscience, 6:917-92

Distinct sulphur saturation histories of the Palaeogene Magilligan Sill, N. Ireland: implications for Ni-Cu-PGE exploration in the North Atlantic

Jordan J. Lindsay, Hannah S. R. Hughes, Jens C. Ø. Andersen
Camborne School of Mines, University of Exeter, UK

Dermot Smyth
Lonmin (Northern Ireland) Ltd., UK

Iain McDonald
School of Earth and Ocean Sciences, Cardiff University, UK

Adrian J. Boyce
SUERC, East Kilbride, Scotland, UK

Abstract. The ~60 m thick Northern Irish Magilligan Sill is a dolerite and olivine gabbro intrusion, thought to be connected to the Irish dyke swarm plumbing system that is part of the British Palaeogene Igneous Province (BPIP) in the North Atlantic. The sill has received interest as an exploration target for Ni-Cu-PGE sulphide mineralisation due to its morphological similarity to Noril'sk-Talnakh (Russia). We present new petrological, geochemical and S-isotope data for the sill, to assess its prospectivity and detail the underlying magmatic plumbing system. Most sulphides in the dolerite portions of the sill contain negligible PGE. In the olivine gabbros, sulphides contain significant PGE, Cu, Ni, Co and Ag. Pyrite from the dolerites have $\delta^{34}S$ ranging from -10.0 to +3.4 ‰ and olivine gabbro sulphides range from -2.5 to -1.1 ‰, suggesting widespread crustal contamination. The S/Se ratios of sulphides in the dolerites and olivine gabbros range from 3,500 to 19,500 and from 1,970 to 3,710, respectively, indicating that olivine gabbro sulphides may have come from upstream in the magma plumbing system. The Magilligan Sill records multiple injections of mafic magma into a single intrusive package, each with distinct mechanisms towards S-saturation. The divergence in S-saturation histories and metal contents suggest that a larger volume of olivine gabbro sulphides at depth may be prospective.

1 Geological Setting

The Magilligan Sill is a mafic intrusion injected into Mesozoic sedimentary rocks on the north coast of County Londonderry, Northern Ireland. It crops out close to the western edge of the Antrim Plateau, and is part of the BPIP in the North Atlantic Igneous Province (NAIP) (GSNI, 2004). Given its setting within a large igneous province, injected through a thick sequence of S-rich crustal sediments (akin to the Siberian Noril'sk Talnakh Ni-Cu-PGE deposit; Arndt et al. 2003), it is an interesting metal exploration target. Lonmin (Northern Ireland) Ltd. and now Walkabout Resources have been investigating the area since 2014. This study is the first published in-depth petrological and geochemical account of the sill since its first documentation (BGS, 1964).

2 Methods

A total of forty-seven half or quarter diamond drill core samples were collected for this study from three Lonmin boreholes in 2017 that intersect the sill and the overlying/underlying Mesozoic sedimentary rocks. The samples were analysed using electron microprobe analysis and laser ablation inductively coupled plasma (LA-ICP-MS) for in-situ major and trace element abundances, including PGE. Sulphur isotope ($\delta^{34}S$) analyses by mineral picking and conventional analysis of sulphides from the sill and sediment samples provide an indication of the S-saturation regime within the sill.

3 Results

New petrological logging of the drill core samples defined two major lithologies in the Magilligan Sill package. The first, which made up the majority of the intrusion thickness (~60 m), is a dolerite to gabbro (referred to herein as 'dolerite' for brevity). Laser ablation work revealed sulphides in the dolerites have a significant or complete lack of base and precious metals including PGE. The second lithology, which occurred as multiple ~1 m horizons within the main lithology, is an olivine gabbro. Chalcopyrite and pentlandite in the olivine gabbro contain up to 4 ppm total PGE, 1,460 ppm Co and 88 ppm Ag. Pyrite from the dolerites display $\delta^{34}S$ ranging from -10.0 to +3.4 ‰, whereas sulphides in the olivine gabbro display signatures ranging from -2.5 to -1.1 ‰, S/Se in the different lithologies varies significantly, with the dolerites recording ratios an order of magnitude higher than the 'mantle-like' values of 2,850 to 4,350 (Eckstrand and Hulbert, 1987). Geochemical data are summarised in Fig. 1

.

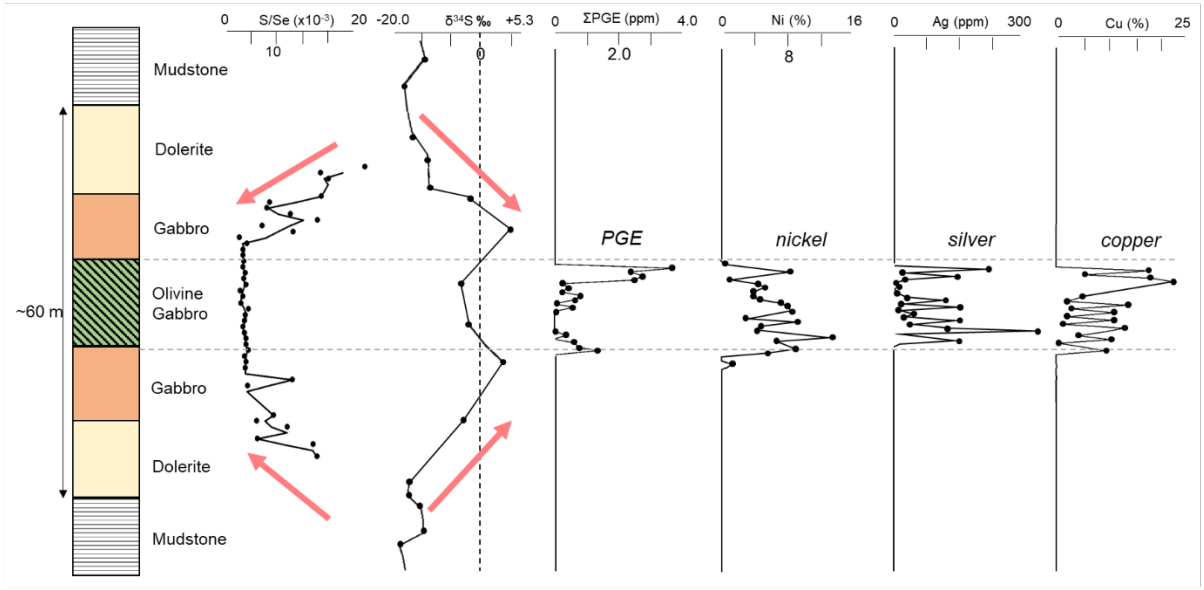

Figure 1. Representative downhole variations in lithology (not to scale) combined with S/Se, $\delta^{34}S$, total PGE, Ni, Ag and Cu data from sulphides in these lithologies. Arrows on S/Se and $\delta^{34}S$ plots describe the suggested diffusion profile grading inwards from dolerite to gabbro.

4 Distinct S-saturation histories

Discrete pulses of at least two chemically distinct magma generations were emplaced into the Magilligan sill within a single intrusion. Sulphur isotope signatures in the sill suggest widespread crustal contamination, given that 'mantle-like' $\delta^{34}S$ should be 0.1 ± 0.5 ‰ (Sakai et al. 1984). The large discrepancy in S/Se among the various horizons suggests that despite widespread contamination, their S-saturation mechanisms were different. The olivine gabbros (with low S/Se) are likely to have had less S added than the dolerites or even had S removed from sulphides through time. Ultimately, the sill appears to be made up of two distinct pulses of magma each with their own petrology, geochemistry, S-saturation pathways and mineralisation potential. The first magmatic generation crystallised to form most of the sill – olivine-deficient dolerites and gabbros with barren sulphide minerals. The second generation crystallised to form olivine gabbro horizons within the pre-existing sill, and contained metal-enriched sulphides. In order to form younger, more primitive magmas, the feeder chamber must have mixed with a new magma between the emplacements of the two different units in the sill, in a similar fashion to the overlying Antrim Plateau Lavas, in which more mafic Upper Basalts postdate less mafic Lower Basalts.

Overall, the $\delta^{34}S$ of the Magilligan Sill indicates that crustal S contamination is present throughout the entire intrusion. S/Se ratios in second-generation (olivine gabbro) sulphides are similar to that of published average 'magmatic' values of 2,850-4,350 (Eckstrand and Hulbert, 1987; Queffurus and Barnes, 2015), indicating a deeper/earlier S-saturation event perhaps with smaller degrees of crustal contamination. We propose that the second generation of sulphides belonging to the olivine gabbros were originally mineralised 'upstream' in the plumbing system that fed the Magilligan Sill. They were cycled through subsequent pulses of second-generation magma before being entrained and emplaced into the Magilligan Sill via 'cumulative R-factor' (Kerr and Leitch, 2005), in which subsequent magma pulses remove S from sulphides caught in the pulse while leaving metals (e.g. Se and PGE).

Figure 2 summarises the perceived development of the Magilligan Sill in 2 phases. The pre-existing dolerites and gabbros formed during Stage A most likely shielded this second pulse of magma (Stage B) from further S absorption from the local country rocks, preventing dilution or addition of late-stage magmatic-hydrothermal S. The possible controls on this deep S-saturation include: the changing initial composition of the magma at source; the amount of sedimentary S available to the magma via assimilation, and the degree of shielding from these sediments enforced by pre-existing layers of the sill; and the geometry of the magmatic plumbing system. Through a combined approach of S-isotopes, S/Se ratios and detailed petrography, the pathways to S-saturation may be determined within plumbing systems and valuable information fed back into the exploration industry with regards to vectoring towards orthomagmatic sulphide mineralisation, both in the BPIP and more generally for large igneous provinces.

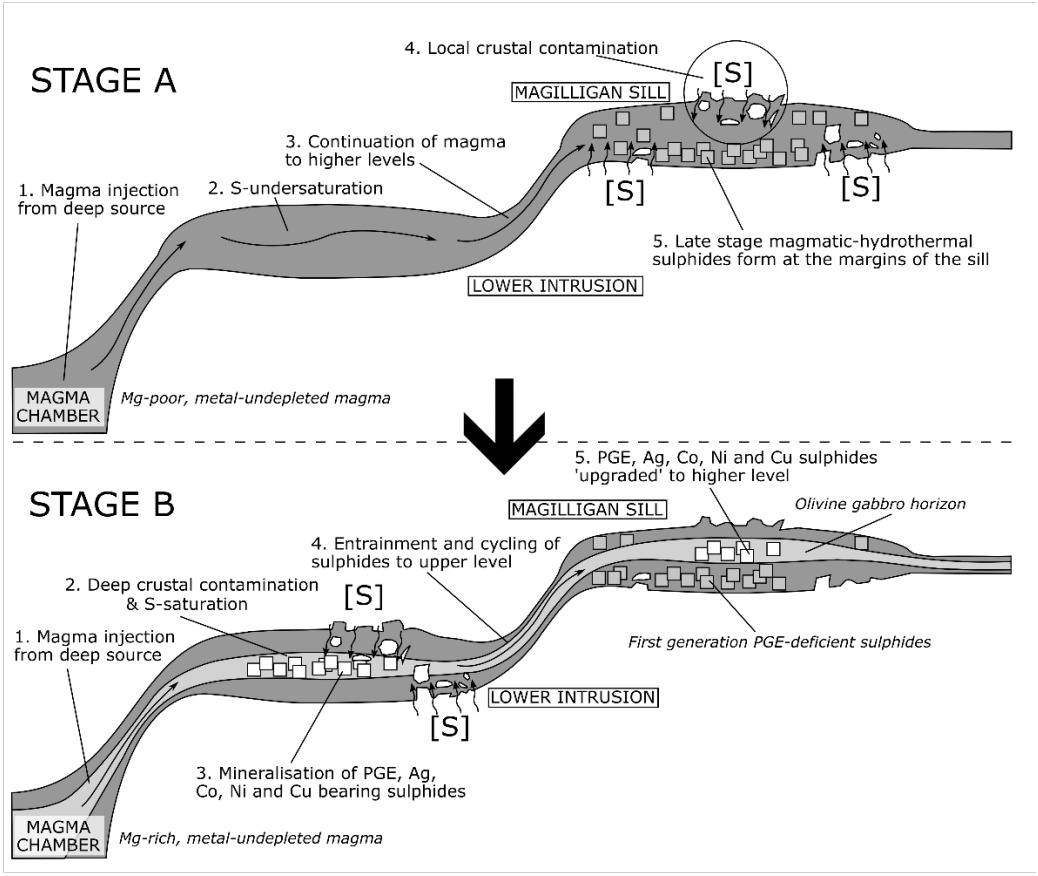

Figure 2. Stage A in the magmatic development model for the Magilligan system, showing the formation of the dolerites and gabbros, and their barren sulphides. Stage B in the magmatic development model for the Magilligan system, showing the formation of the olivine gabbros, and their cycled base/precious metal sulphides. Model constructed with reference to similar systems in Barnes et al. (2016)

Acknowledgements

The authors would like to thank Gavyn Rollinson, Peter Frost, Joe Pickles, and Charlie Compton-Jones at the Camborne School of Mines laboratory facilities for their guidance during SEM and EPMA analyses. Thanks are also extended to Alison McDonald of the Scottish Universities Environmental Research Centre (SUERC) for her assistance on sulphur isotope analysis, and to Lonmin (Northern Ireland) Ltd. for access to core and previous studies on the sill. Walkabout Resources are thanked for their support in publishing this work and for access to company data.

References

Arndt, N.T., Czamanske, G.K., Walker, R.J., Chauvel, C., Fedorenko, V. a., 2003. Geochemistry and Origin of the Intrusive Hosts of the Noril'sk-TalnakhCu-Ni-PGE Sulfide Deposits. Econ. Geol. 98:495–515. https://doi.org/10.2113/gsecongeo.98.3.495

Barnes, S.J., Cruden, A.R., Arndt, N., Saumur, B.M., 2016. The mineral system approach applied to magmatic Ni–Cu–PGE sulphide deposits. Ore Geol. Rev. 76:296–316. https://doi.org/10.1016/j.oregeorev.2015.06.012

BGS, 1964. Summary of progress of the Geological Survey of Great Britain and the Museum of Practical Geology for the year 1963. HMSO, London.

Eckstrand, O.R., Hulbert, L.J., 1987. Selenium and the source of sulfur in magmatic nickel and platinum deposits. Geol. Assoc. Canada –Mineralogical Assoc. Canada Progr. with Abstr. 12, 40.

GSNI, 2004. The Geology of Northern Ireland - Our Natural Foundation, 2nd ed. Crown, Belfast.

Kerr, A.C., Leitch, A.M., 2005. Self-destructive sulfide segregation systems and the formation of high-grade magmatic ore deposits. Econ. Geol. 100:311–332. https://doi.org/10.2113/gsecongeo.100.2.311

Queffurus, M., Barnes, S.J., 2015. A review of sulfur to selenium ratios in magmatic nickel-copper and platinum-group element deposits. Ore Geol. Rev. 69:301–324. https://doi.org/10.1016/j.oregeorev.2015.02.019

Sakai, H., Marais, D.J.D., Ueda, A., Moore, J.G., 1984. Concentrations and isotope ratios of carbon, nitrogen and sulfur in ocean-floor basalts. Geochim. Cosmochim. Acta 48:2433–2441. https://doi.org/10.1016/0016-7037(84)90295-3

Thermal modelling of the Paleoproterozoic Fedorova layered intrusion, Kola Region, Russia: implications for the origin of contact-style PGE mineralisation

Nikolay Yu. Groshev, Dmitriy G. Stepenshchikov,
Geological Institute, Kola Science Centre, Russian Academy of Sciences, Russia

Bartosz T. Karykowski
Fugro Germany Land GmbH, Resource Consulting, Germany

Malte Junge
Institute of Earth and Environmental Sciences, University Freiburg, Germany

Artyom M. Sushchenko
Murmansk State Technical University, Russia

Abstract. This contribution presents the results of thermal modelling of the Paleoproterozoic Fedorova intrusion located in the central part of the Kola Peninsula, NW Russia. The intrusion hosts a large contact-style platinum-group elements (PGE) deposit in its basal 300-m-thick unit (Fedorova Tundra). This basal unit is composed of varied-textured gabbronorite and is believed to be an additional injection of sulphide-saturated magma, representing a second intrusive phase. The irregular distribution of sulphides across the entire basal unit and the absence of sulphide liquid migration into the underlying basement rocks suggest that this second injection exploited the cooled down contact between the first intrusive phase and the basement. The hiatus between the first and the second intrusive event allowed for some cooling of the former, however, the duration of the hiatus remains unknown. Assuming an average geothermal gradient of 30°C/km and a basement temperature of approx. 400°C due to preheating, thermal modelling indicates that the hiatus may have lasted for some 600–700 thousand years. These results are in agreement with a classic contact-style PGE mineralisation model for Fedorova Tundra and suggest an *out-of-sequence* formation of the layered succession.

1 Introduction

A critical factor in the formation of contact-style low-sulphide platinum group elements (PGE) mineralisation in layered mafic-ultramafic intrusions is the preheating of host rocks due to magmatic activity, preceding the emplacement of sulphide-saturated magma (Karykowski et al. 2018). Preheating of the basement to 400 °C by the intrusion of, for example, a series of dikes or sills that precede the main intrusion, creates conditions for the effective accumulation of sulphide droplets at the bottom of the magma chamber as well as for the percolation of sulphide droplets into the partially molten basement rocks. The Paleoproterozoic Portimo and Monchegorsk layered complexes on the Fennoscandian Shield are typical examples of intrusions where this factor played a crucial role (Iljina 1994; Karykowski et al. 2018).

The Fedorova intrusion represents the western block of the Paleoproterozoic Fedorova-Pana Complex located in the central part of the Kola Peninsula, NW Russia. The intrusion forms a 4-km-thick lens-like body that is steeply dipping to the southwest (Fig. 1a). Three zones are distinguished in the sequence of the Fedorova intrusion (from the bottom upwards): a Norite-Gabbronorite Zone (or 'basal unit'), a Leucogabbro-Gabbronorite Zone, and a Leucogabbro Zone (Staritsina 1978). It is suggested that the Leucogabbro-Gabbronorite and the Leucogabbro zones comprise an early magmatic phase (2526-2515 Ma) with reef-style PGE mineralization, whereas the contact-style PGE mineralisation-hosting basal unit belongs to a later intrusive phase (2493-2485 Ma) (Schissel et al. 2002; Groshev et al. 2009; Groshev and Savchenko 2011). The 300-m-thick basal unit is composed of varied-textured melanorite and gabbronorite containing abundant orthopyroxenitic autoliths and irregular patches of disseminated sulphide enriched in PGE (2–5 vol. %) (Fig. 1, b). Evenly disseminated sulphide accumulations (20–30 vol. %) are generally rare, whereas massive sulphides are absent. The PGE mineralisation is only hosted by the basal unit of the intrusion, showing no evidence for sulphide liquid percolation into the basement rocks. These sulphides form the Fedorova Tundra deposit with a total resources of more than 400 t of PGE (Rasilainen et al. 2010).

It is believed that the first intrusive phase of the Fedorova intrusion preheated the basement before the second phase intruded along the lower contact of the first intrusive phase (Fig. 1). A thermal contact aureole of the first phase reaches several hundred meters as evidenced by partially molten two-pyroxene diorites observed in some drill holes (Groshev et al. 2009). In spite of this the second intrusive phase does not practically show features of sulphide accumulation within the basal unit or sulphide percolation into the basement rocks. Consequently, the time gab between the intrusive phases was long enough for cooling of the basement below

400 °C (temperature supporting sulphide migration and accumulation). The purpose of this study is to estimate the time gap between the two intrusive phases comprising the Fedorova intrusion using thermal modelling and to discuss the results in the context of the crystallization duration of layered intrusions as well as the formation of a contact-style PGE mineralisation.

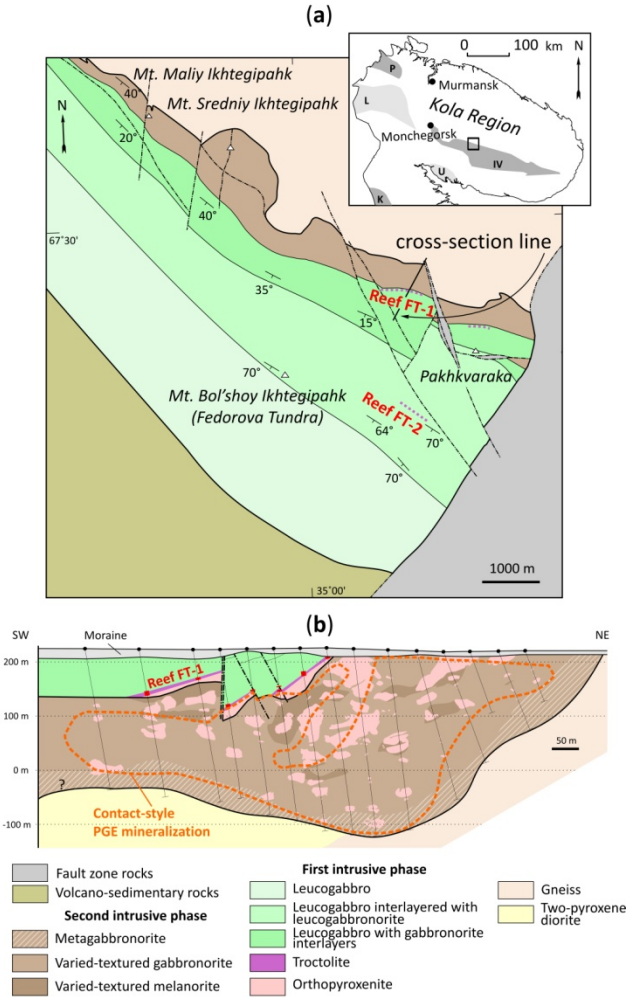

Figure 1. Simplified geologic map of the Fedorova Tundra intrusion (a) and schematic geologic cross section through the deposit (b). Purple dotted lines show a position of PGE reefs (FT-1 and FT-2) on the map; red rectangles on the cross section indicate mineralized intervals of the FT-1 Reef. Proterozoic structures of the predominantly Archean Kola Region (inset): Imandra-Varzuga (IV), Kuolajarvi (K), and Pechenga (P) paleorift structures; Lapland (L) and Umba (U) granulite belts. Modified after (Groshev and Savchenko 2011).

2 Methods

The cooling of the first intrusive phase of the Fedorova massif can be modelled by heat exchange between the magmatic succession with a temperature of 1200 ° C, which has intruded the Archean basement at a depth of 5 km (Dubrovskiy and Rundkvist 2008). The thickness of the body is assumed to be 4 km (Groshev and Savchenko 2011). Discretisation of the one-dimensional heat equation gives the following recurrence formula:

$$T_i^{n+1} = T_i^n + k\Delta t\left(\frac{T_{i+1}^n - 2T_i^n + T_{i-1}^n}{(\Delta x)^2}\right),$$

where k – thermal diffusivity (k = 2·10^{-6} m^{2}s^{-1}), and T_i^n – temperature at a depth of $i{\cdot}\Delta x$ m in $n{\cdot}\Delta t$ years. A detailed derivation of the equation is given in (Karykowski et al. 2018). To eliminate boundary effects, the depth of modelling was increased to 20 km.

The thermal modelling was carried out using a FPC-based software (Stepenshchikov and Groshev 2019). Intrusive bodies are defined by four parameters: the boundary of the roof (m), thickness (m), temperature (°C) and the point in time of intrusion (years). One can set a number of intrusive bodies at different moments of time. For each body, the modelling parameters are printed in a single line in window 1 of the software interface (Fig. 2). During the simulation, the current time and the moments of emplacement are comparing and when they match, temperature of intrusive body assigns to corresponding depths. Then the calculation procedure continues.

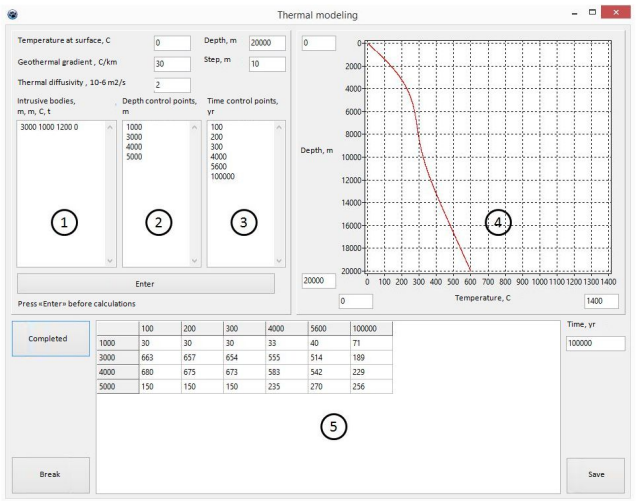

Figure 2. Software interface. 1 – parameters of intrusions, 2 – temperature control depths, 3 – temperature control points, 4 – temperature-depth graph, 5 – temperature table for given depths and time points (window 2 and 3).

To track the temperature profile with depth and time, one can set a list of depths (window 2 in Fig. 2) and time points (window 3 in Fig. 2). They will be automatically reordered and rewrited in the corresponding windows. Based on these data, a table of temperatures is created (window 5 in Fig. 2). This table can then be exported into an .xls-file. The temperature-depth plot for time points from window 3 are showing in window 4. This window may also be useful for testing the validity of the input parameters. The simulation time is limited by the last time point in window 3. An early stop of simulation is provided and after an interruption of the calculation, the modelling will start anew without saving previous results.

3 Thermal modelling results

The simulation shows that the emplacement of the Fedorova first phase will lead to a significant heating of

the underlying rocks (Fig. 3 a–c; Table 1). The partial melting temperature of the basement (≈ 700 °C) will be

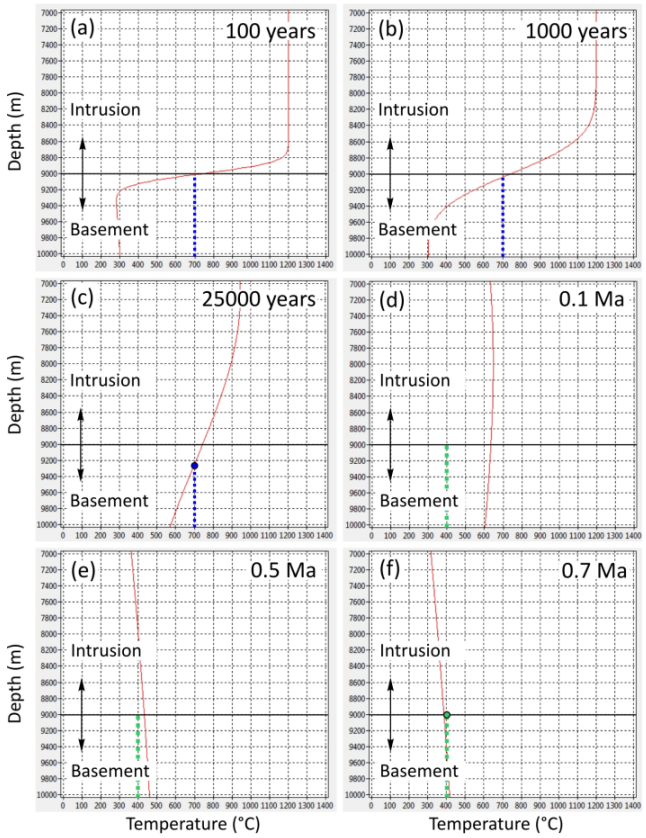

Figure 3. Temperature-depth graphs showing changes in temperature (red line) near the lower contact of the first intrusive phase of the Fedorova intrusion for different time moments (a–f). Note that an intrusion of the second phase could occur only after a contact cooling to 400 °C (green circle).

reached approx. 250 m away from the lower intrusion contact after some 25 thousand years (Fig. 3 c, blue circle). This is in agreement with the thickness of two-pyroxene diorite below the intrusion (Fig. 1 b).

Since the magma of the second intrusive phase was sulphide-saturated, as a result of its emplacement in the preheated by the first phase contact with the basement the sulphides would have been concentrated near the bottom of the intrusion forming sulphide-rich layers and locally percolating into the Archean gneissic basement. Fig. 1 b shows that sulphides distributed unevenly and the migration of sulphide liquid is not observed at the Fedorova Tundra deposit. Consequently, the basal unit consisting of varied-textured gabbronorite that postdate the first intrusive phase were emplaced after the temperature at the lower contact of the first phase reached less than 400 °C. Under these boundary conditions, the minimum time separating the different intrusive phases is some 600–700 thousand years, as can be seen in Fig. 3 e–f (green circle) and Table 1.

4 Discussion

4.1 Duration of the Fedorova intrusion crystallization

The example of the Fedorova intrusion shows that the duration of crystallization under open-system conditions can be hundreds of thousands of years (Fig. 3). At the same time, the latest data on systematic isotope dating of open-system layered intrusions, show that the duration of their crystallization ranges from 1 to 3 Ma with an error of individual age determinations of up to 0.26 Ma modulo (Scoates and Wall 2015; Zeh et al. 2015; Wall et al. 2018). In this regard, it is worth noting that the currently available geochronological data on the Fedorova intrusion suggest a duration of crystallisation spanning some 40 Ma (Groshev et al. 2009), which appears to be greatly overestimated due to the likely inclusion of secondary zircon in the calculation of U-Pb ages (Groshev and Karykowski 2019).

Table 1. Thermal modelling results for the first phase of the Fedorova intrusion.

t (years)	Temperature, T (°C)	
	d=5 km	d=9 km
1	839	880
10	732	787
100	692	753
1000	677	744
10000	663	750
100000	517	635
200000	415	551
300000	350	500
400000	306	462
500000	276	431
600000	254	407
700000	236	386
800000	223	369
900000	211	355
1000000	202	342

Thus, the Fedorova Tundra deposit most likely represents a separate ‘out-of-sequence’-type of contact-style PGE mineralization. The advancement of the isotope age determination on the intrusive phases of the Fedorova intrusion is possibly one of the most important unresolved problems in the petrology of layered intrusions on the Fennoscandian Shield.

4.2 Similar contact-style PGE mineralization in other layered intrusions

The presence or absence of sulphide liquid migration from the basal mineralised zones into the basement rocks is an important genetic feature of contact-style PGE deposits, revealing their thermal history. Except the Fedorova intrusion it can be shown by thermal modeling for the Nyud-Poaz massif (Monchegorsk Complex), which has two ore-bearing intrusive phases both containing disseminated sulfides, extending beyond the intrusion in the basement (Karykowski et al. 2018; Groshev and Pripachkin 2018). An additional phase (Gabbro-10), emplaced along the basal contact of the Nyud-Poaz intrusion hosts PGE mineralisation that percolates into the Archean basement for 30 m. Consequently, the additional injection of sulphide-saturated magma occurred at a time when the basal contact of the Nyud-Poaz massif was characterised by elevated temperatures. The time gap between these two phases, according to the thermal modelling of the Nyud-Poaz massif, is no more than 150 thousand years. The accuracy of isotope dating cannot resolve such small time differences at the moment (Scoates and Wall 2015). This is also shown by the isotope dating of the Gabbro-10 intrusion whose age coincides with the age of the Nyud-Poaz massif within the error limits (Amelin et al. 1995; Groshev et al. 2018).

The South Sopcha intrusion of the Monchegorsk Complex is another example of contact-style PGE mineralisation that was likely formed out-of-sequence (Chashchin and Mitrofanov 2015; Pripachkin et al. 2015). The South Sopcha intrusion has an orthopyroxenitic lower unit, which is extensively intruded and brecciated by sill-like gabbro-pegmatites and coarse-grained gabbronorites containing PGE-rich disseminated sulphide. The issues of sulphide migration from the gabbronorites into the basement rocks as well as the duration of the South Sopcha crystallisation are to be solved in future research.

Acknowledgements

This research was carried out under the scientific theme No. 0226-2019-0053.

References

Amelin YV, Heaman LM, Semenov VS (1995) U-Pb geochronology of layered mafic intrusions in the eastern Baltic Shield: implications for the timing and duration of Paleoproterozoic continental rifting. Precambrian Res 75:31–46. doi: 10.1016/0301-9268(95)00015-W

Chashchin VV, Mitrofanov FP (2015) The Paleoproterozoic Imandra-Varzuga Rifting Structure (Kola Peninsula): Intrusive Magmatism and Minerageny. Geodin i Tektonofiz 5:231–256

Dubrovskiy MI, Rundkvist TV (2008) Petrology of the Early Proterozoic platinum-bearing Fedorova tundras massif (Kola Peninsula). Zap RMO CXXXVII:20–33

Groshev NY, Karykowski BT (2019) The Main Anorthosite Layer of the West-Pana Intrusion, Kola Region: Geology and U-Pb Age Dating. Minerals 9:71. doi: 10.3390/min9020071

Groshev NY, Nitkina EA, Mitrofanov FP (2009) Two-phase mechanism of the formation of platinum-metal basites of the Fedorova Tundra intrusion on the Kola Peninsula: New data on geology and isotope geochronology. Dokl Earth Sci 427:1012–1016. doi: 10.1134/S1028334X09060270

Groshev NY, Pripachkin PV, Karykowski BT, et al (2018) Genesis of a Magnetite Layer in the Gabbro-10 Intrusion, Monchegorsk Complex, Kola Region: U–Pb SHRIMP-II Dating of Metadiorites. Geol Ore Depos 60:486–496. doi: 10.1134/s1075701518060028

Groshev NY, Savchenko EE (2011) Invisible Reef - a new horizon of low-sulfide PGE mineralization in the Fedorova Tundra massif, Kola Peninsula. Rudy Met 5:5–26

Iljina M (1994) The Portimo layered igneous complex: with emphasis on diverse sulphide and platinum-group element deposits. University of Oulu Oulu, Finland

Karykowski BT, Maier WD, Groshev NY, et al (2018) Critical controls on the formation of contact-style PGE-Ni-Cu mineralization: Evidence from the paleoproterozoic Monchegorsk Complex, Kola Region, Russia. Econ Geol 113:911–935. doi: 10.5382/econgeo.2018.4576

Pripachkin PV, Rundkvist TV, Miroshnikova YA, et al (2015) Geological structure and ore mineralization of the South Sopchinsky and Gabbro-10 massifs and the Moroshkovoe Lake target, Monchegorsk area, Kola Peninsula, Russia. Miner Depos 973–992. doi: 10.1007/s00126-015-0605-0

Rasilainen K, Eilu P, Halkoaho T, et al (2010) Quantitative mineral resource assessment of undiscovered PGE resources in Finland. Ore Geol Rev 38:270–287. doi: 10.1016/j.oregeorev.2010.05.001

Schissel D, Tsvetkov AA, Mitrofanov FP, Korchagin AU (2002) Basal Platinum-Group Element Mineralization in the Federov Pansky Layered Mafic Intrusion, Kola Peninsula, Russia. Econ Geol 97:1657–1677. doi: 10.2113/gsecongeo.97.8.1657

Scoates JS, Wall CJ (2015) Geochronology of Layered Intrusions. In: Charlier B (ed) Layered Intrusions. Springer Netherlands, Dordrecht, pp 3–74

Staritsina GN (1978) Fedorova Tundra massif of basic-ultrabasic rocks. In: Issues of geology and mineralogy, Kola Peninsula. Apatity, Kola Branch AS USSR, pp 50–91

Stepenshchikov DG, Groshev NY (2019) The application software for thermal modeling of intrusions. Tr FNS 16:in press

Wall CJ, Scoates JS, Weis D, et al (2018) The Stillwater Complex: Integrating Zircon Geochronological and Geochemical Constraints on the Age, Emplacement History and Crystallization of a Large, Open-System Layered Intrusion. J Petrol 59:153–190

Zeh A, Ovtcharova M, Wilson AH, Schaltegger U (2015) The Bushveld Complex was emplaced and cooled in less than one million years - results of zirconology, and geotectonic implications. Earth Planet Sci Lett 418:103–114. doi: 10.1016/j.epsl.2015.02.035

Sulfide textures, chalcophile element distribution, and timing of mineralization within the Crystal Lake intrusion, 1.1 Ga Midcontinent Rift

Jennifer W. Smith, Wouter Bleeker, Duane Petts
Geological Survey of Canada

Mike Hamilton
Jack Satterly Geochronology Laboratory, University of Toronto

Abstract. Magmatic Ni-Cu-PGE deposits of the ca. 1.1 Ga Midcontinent Rift (MCR) occur in association with a diverse range of ultramafic-mafic intrusions. High precision U-Pb dating throughout the MCR is critical for constraining the various magmatic pulses, the temporal and spatial controls on metal enrichment, and improving our general understanding of the rift's evolution. The 1099 Ma Crystal Lake layered intrusion is an olivine rich, Cr-spinel bearing, vari-textured gabbroic body, that hosts extensive low-grade Ni-Cu-PGE mineralization, and is broadly comparable to the nearby Duluth Complex. The Ni-Cu-PGE mineralization shows some similarities to other deposits such as Marathon (Coldwell Complex), Voisey's Bay and Norilsk. Segregation vesicles are common and show a close association with globular sulfides. The timing, cause and significance of degassing for ore genesis is yet to be fully explored but appears to be a feature of many Ni-Cu deposits.

1 Introduction

North America's Midcontinent Rift (MCR) represents one of the best preserved and accessible intra-continental rift systems of late Mesoproterozoic age. The ca. 1.1 Ga failed rift system hosts a range of mafic-ultramafic, carbonatitic and alkaline intrusions, many of which are actively being explored for a range of commodities (e.g. Ni, Cu, PGE, Co, Cr, V, Nb). The magmatic Ni-Cu-PGE sulfide deposits occur in association with a diverse range of mafic and mafic-ultramafic intrusions. Like many other world-class Ni-Cu deposits (e.g. Norilsk, Voisey's Bay, Raglan), this mineralization shows a close spatial and temporal relationship with large volumes of magma erupted at or near the margins of Archean cratons (Begg et al. 2010; Barnes et al. 2016) and a local prolific sulfur source.

Within the MCR, the most prospective Ni-Cu-PGE targets (e.g. Eagle, Tamarack) are hosted by small, 'early-rift' (ca. 1117–1106 Ma; Miller and Nicholson 2013), mafic-ultramafic intrusions. These deposits are developed within the magmatic plumbing system of the rift, an environment known to be favourable for the development of high-grade massive sulfides (Song et al. 2011; Barnes et al. 2016). The ca. 1099 Ma Duluth Complex and similar large, sill-like, mafic layered intrusions (e.g. Sonju Lake, Mellen Complex, Echo Lake, Crystal Lake, Coldwell Complex) are also known to host Ni-Cu-PGE sulfide mineralization (Good and Crocket 1994; Joslin 2004; Ripley 2014). Although these intrusion types are characterized by disseminated sulfides and often have lower grades than the conduit deposits, they remain prospective targets and are favourable settings for the development of stratiform reef-style PGE-Ni-Cu mineralization (e.g. Sonju Lake: Joslin 2004; and Duluth Complex: Miller 1998).

Although the MCR system has a rich legacy of past and on-going research, the fundamental controls pertaining to the localization and timing of mineralization remain poorly understood. In order to understand why significant Ni-Cu-PGE mineralization is not developed within all rift-related mafic-ultramafic intrusions a better temporal framework in addition to an improved understanding of source characteristics and geometry is required.

2 Crystal Lake intrusion

A detailed geochemical and isotopic study is underway on the 1099.1 ± 1.2 Ma (Heaman et al. 2007) Crystal Lake intrusion, which has previously been compared to the proximal Duluth Complex (Thomas 2015). The aim of this study is to gain further insights into the controls on ore genesis within the 'main-rift' intrusions (Miller and Nicholson 2013).

The Crystal Lake intrusion, located 47 km southwest of Thunder Bay, Ontario, Canada, outcrops as a prominent Y-shaped body (Fig. 1) within the Paleoproterozoic Animikie basin, intruding sulfur-bearing shale, argillite and greywacke of the Rove Formation (Geul 1970, 1973). Geochemically, the Crystal Lake intrusion can be distinguished from the more primitive conduit-type bodies by its olivine composition (Fo51-79), lower Ni/Cu and Pt/Pd ratios (<1), higher rare earth element (REE) abundances, light REE enrichment and minimal fractionation of heavy REEs (Gd/Yb <2; Thomas 2015; O'Brien 2018).

Although a number of dating studies have been undertaken on the MCR (see Heaman et al. 2007, for a relatively recent compilation), many of the intrusions either lack the precision that is now possible with routine chemical abrasion U-Pb geochronology or are yet to be dated. Consequently, the relationship between various rift-related intrusions remains poorly constrained. We are currently undertaking a comprehensive geochronology

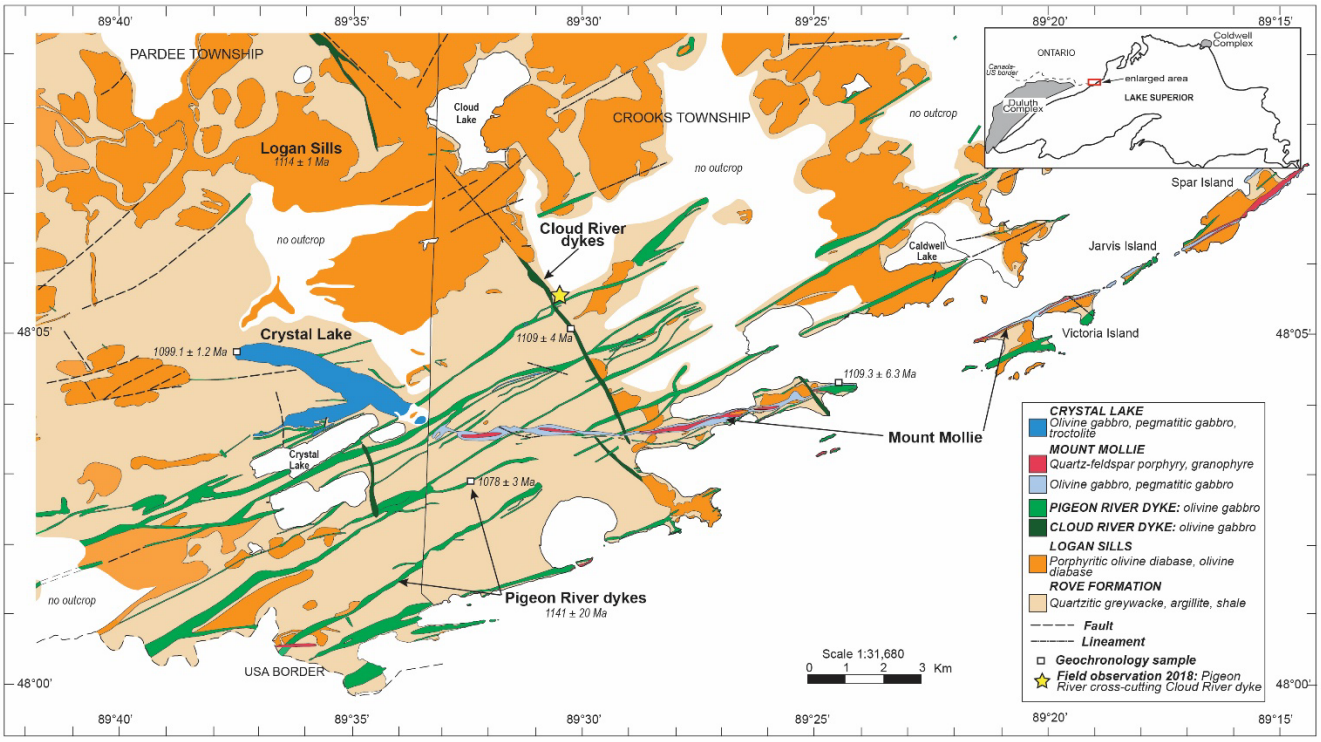

Figure 1. Geological map of the Pardee and Crook townships showing the location of Crystal Lake, Mount Mollie and the Pigeon River and Cloud River dyke sets. Modified from Geul 1970, 1973. U-Pb ages taken from Heaman et al. (2007) and Hollings et al. (2010)

study throughout the MCR, this includes detailed dating of the Crystal Lake intrusion. In addition to refining Heaman's et al. (2007) baddeleyite age of 1099.1 ± 1.2 Ma we aim to constrain the relationship of the northern and southern limbs of the intrusion. Furthermore, we plan to untangle the timing of the Crystal Lake intrusion relative to other MCR intrusive events including the NE-trending Pigeon River dykes, the NW-trending Cloud River dykes and the sulfide-bearing Mount Mollie intrusion developed to the east (Fig. 1).

Crystal Lake has previously been suggested to be coeval with the Mount Mollie dyke (Smith and Sutcliffe 1987; O'Brien 2018). This however is not supported by the current baddeleyite age date of 1109.3 ± 6.3 Ma (Hollings et al. 2010). Due to limited exposure, the timing relationships of the Crystal Lake intrusion with the Pigeon River, Mount Mollie and Cloud River dykes has not been successfully established from field observations.

3 Ni-Cu-PGE mineralization

Ni-Cu-PGE sulfide mineralization is developed within the northern and southern limbs of the Crystal Lake intrusion in association with vari-textured gabbros and irregular Cr-spinel-bearing horizons (Fig. 2). The association of sulfides and metal enrichment with pegmatitic/taxitic units is also observed within other Ni-Cu-PGE deposits such as the ca. 1108 Ma (Heaman and Machado 1992) Coldwell Complex, Merensky Reef, Norilsk and Voisey's Bay. The upper troctolite and magnetite-bearing olivine gabbro of the northern and southern limbs, respectively, appear to be barren of sulfides.

Sulfide mineralization is largely disseminated, with massive sulfides (<50 cm in thickness) developed locally within the northern limb (Fig. 2). The disseminated ores are variable in texture with globular (capped and uncapped), blebby and interstitial sulfides identified. Within the Crystal Lake intrusion, globular sulfides have been identified within the mineralized zones of the southern limb, where they occur in association with both the vari-textured gabbros and Cr-spinel-bearing ores. Disseminated sulfide ores within the northern limb appear to be more interstitial and blebby in morphology.

Silicate-capped sulfide globules have been recognized in other Ni-Cu sulfide deposits (e.g. Norilsk, Insizwa Complex; Barnes et al. 2017; Le Vaillant et al. 2017) and are interpreted as being the remnants of former segregation vesicles that attached to an immiscible sulfide melt (Mungall et al. 2015). Within the Crystal Lake intrusion, the morphology of the caps, which are comprised of amphiboles, clays, chlorite and calcite, is variable. Convex silicate caps, identical to those modelled by Mungall et al. (2015), are present along with very irregular silicate attachments (Fig. 3).

The ores are dominated by the primary magmatic assemblage pyrrhotite, pentlandite, chalcopyrite and cubanite with minor magnetite. Minor nickel arsenides are recognized within the massive sulfide assemblage, where they reside as rounded grains (<150 µm in diameter) within the primary phases. Within the disseminated ores, sulfide grains are composed primarily of either pyrrhotite or chalcopyrite. Pentlandite occurs as granular grains within pyrrhotite, around the margins of the composite grains or along the contact between pyrrhotite and chalcopyrite. Exsolution flames of pentlandite within pyrrhotite are also observed and are preferentially

concentrated along fractures. In areas where chalcopyrite and cubanite occur adjacent to pyrrhotite, rounded relics of pyrrhotite are observed within the Cu-rich phases.

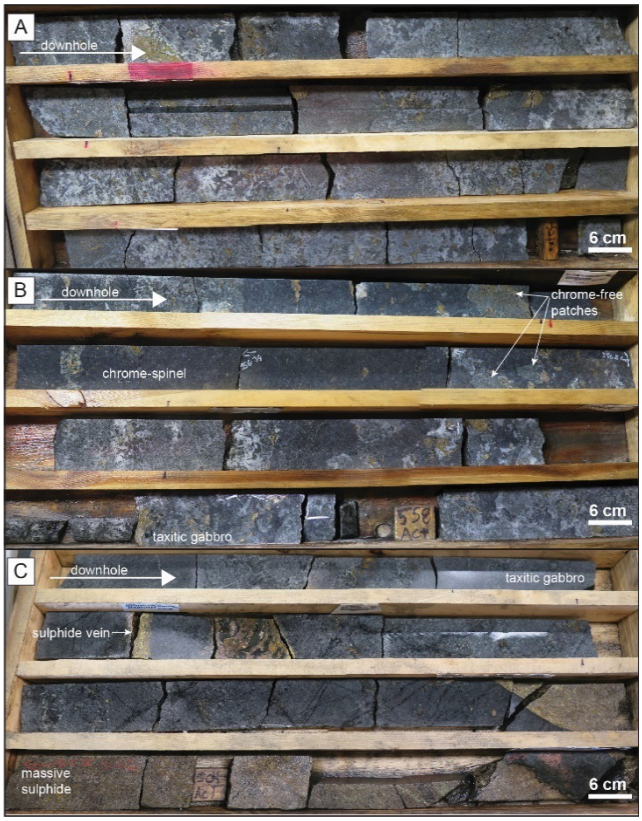

Figure 2. Photographs from the Crystal Lake intrusion. **a.** Vari-textured gabbro. **b.** Horizons rich in Cr-spinel with disseminated and blebby sulfides. **c.** Massive sulfides.

A low temperature alteration assemblage characterized by pyrite, chalcopyrite and magnetite is recognized in both the disseminated and massive sulfide ores. The degree of replacement of the primary assemblage is variable throughout the intrusion although alteration does appear more pervasive in the disseminated ores of the northern limb.

A detailed elemental deportment study is currently in progress, focused on characterizing the distribution and mineralogy of platinum-group minerals (PGMs). Element mapping of sulfides by LA-ICP-MS has been used to further investigate the controls on the distribution of the chalcophile elements during sulfide fractionation. Preliminary observations indicate that Pd resides in solid solution within pentlandite (1-150 ppm) and as small As-Bi and Sb-bearing PGMs. Within the massive sulfides, Pd-bearing minerals show a strong association with nickel arsenides resulting in lower concentrations of Pd (~1 ppm) in the pentlandite than typical of other sulfide assemblages (10–150 ppm). Platinum is not compatible in any of the sulfide phases, instead occurring as discrete As and Sb-bearing PGMs. A close spatial association is observed between the PGMs and the sulfides. The PGMs are found either enclosed or attached to sulfides or within secondary silicates around the altered margins of the sulfides. It is yet to be established whether the crystallization of Cr-spinel and/or low-temperature alteration of the sulfides has had any control on the mineralogy and distribution of PGEs.

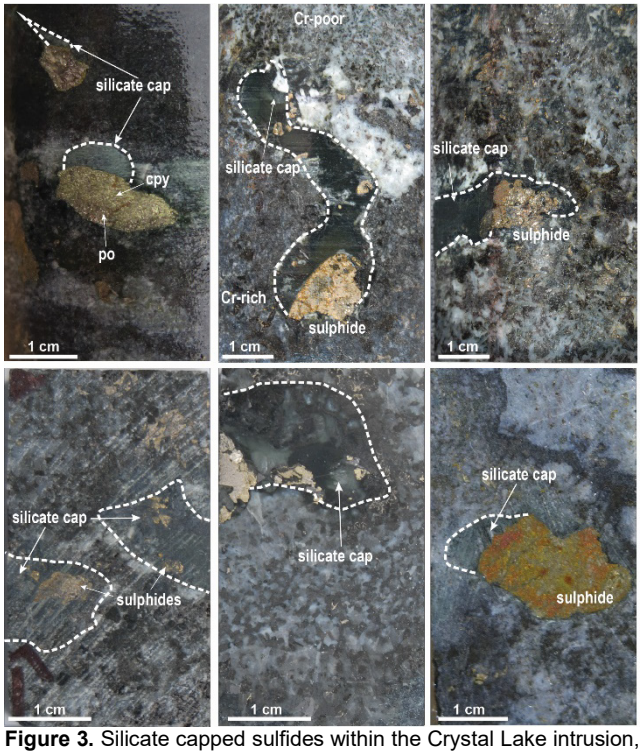

Figure 3. Silicate capped sulfides within the Crystal Lake intrusion, showing a range of sulfide and cap morphologies.

Element mapping of the sulfides by LA-ICP-MS has revealed some interesting structural and/or mineralogical controls on the distribution of chalcophile elements. Although not observed throughout the primary sulfide assemblage, some unaltered sulfides are characterized by a strong microfabric (Fig. 4). This fabric is defined by several elements including As, Mo, Bi, Pb, Pd and Re which appear to be preferentially concentrated along thin, parallel linear features within the pyrrhotite-pentlandite-chalcopyrite assemblage. The molybdenum map also shows thicker banding and elevated concentrations within pyrrhotite (Fig. 4). Interestingly this fabric is not confined to a particular sulfide phase. This is best shown by As, Mo and Re which clearly cut across the boundaries of pyrrhotite, pentlandite and chalcopyrite, which suggests that this fabric was developed subsequent to crystallization of all three sulfide phases. For other elements such as Pd and Pb, the fabric is restricted to the pyrrhotite and pentlandite (Fig. 4). Silicate infilled fractures appear to cut the fabric as shown in the As map. Further work is in progress to determine the controls on selected element mobility (i.e. low temperature alteration or deformation) and to gain an understanding at what scale this remobilization is occurring. If various elements are remobilized over long distances then it could have implications for vectoring of Ni-Cu ore systems.

4 Implications

The MCR provides a superb laboratory to study the differences between mineralized and unmineralized intrusions within a single tectonic setting and provides the opportunity to assess key controls on metal endowment within a LIP-scale magmatic system. Refining and expanding the existing age database for the MCR is fundamental if we are to improve our understanding of the rift's evolution and decipher whether there are temporal and/or spatial controls on metal enrichment. Improved geochronology for intrusions such as Crystal Lake, may also have direct implications for exploration within the area, and help in identifying new prospective intrusions.

Segregation vesicles associated with globular sulfides have recently been recognized in numerous Ni-Cu-PGE bearing mafic intrusions. Those documented at Crystal Lake show a striking resemblance to those described in the Norilsk ores (Le Vaillant et al. 2017; Barnes et al. 2017). The implications of degassing, which appears to be a common process within the Ni-Cu ore systems, for sulfide transportation and deposition is yet to be constrained. Furthermore, the cause (e.g. contamination, pressure changes) and timing of degassing relative to crystallization is not well understood.

Element mapping by LA-ICP-MS is an extremely powerful tool, providing unparalleled detail at the micro scale. This technique provides insight into the behavior and mobility of chalcophile elements during sulfide fractionation, low temperature alteration and/or deformation and may provide a link to larger element haloes associated with some Ni-Cu-PGE deposits.

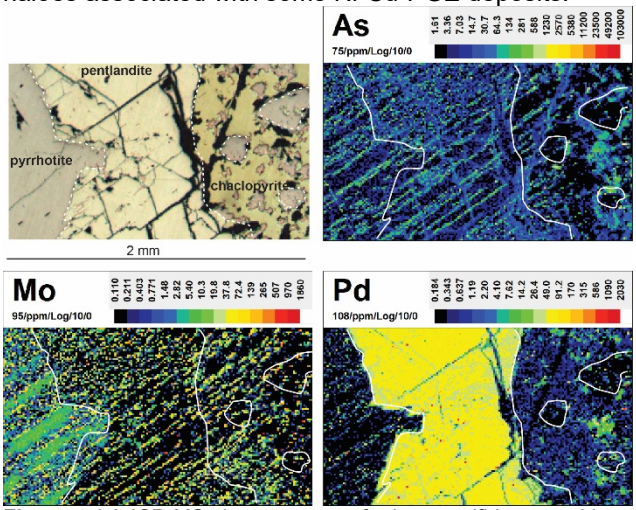

Figure 4. LA-ICP-MS element maps of primary sulfide assemblage.

Acknowledgements

This study was supported by the Geological Survey of Canada's Targeted Geoscience Initiative Program (TGI). The authors thank our partners at Rio Tinto, North American Palladium, Transition Metals, Panoramic, Stillwater Canada and Lakehead University for their help, access to data and constructive discussions. The Ontario Geological Survey are also thanked for their logistical support throughout the 2017/2018 field season. Sarah Davey is thanked for assistance in the field.

References

Barnes SJ, Cruden AR, Arndt N, Saumur BM (2016) The mineral system approach applied to magmatic Ni–Cu–PGE sulphide deposits. Ore Geology Reviews 76:296–316.

Barnes SJ, Mungall J, Le Vaillant M, Godel B, Lesher M, Holwell D, Lightfoot P, Krivolutskaya N, Wei B (2017) Sulphide-silicate textures in magmatic Ni-Cu-PGE sulphide ore deposits: Disseminated and net-textured ores. American Mineralogist 102:473–506.

Begg GC, Hronsky JA, Arndt NT, Griffin WL, O'Reilly SY, Hayward N (2010) Lithospheric, cratonic, and geodynamic setting of Ni-Cu-PGE sulphide deposits. Economic Geology 105:1057–1070.

Geul JC (1970) Geology of Devon and Pardee Townships and the Stuart Location. Ontario Department of Mines, Geological Report 87.

Geul JC (1973) Geology of Crooks Township, Jarvis and Prince Locations, and Off-shore Islands, District of Thunder Bay. Ontario Department of Mines, Geological Report 102.

Good DJ Crocket JH (1994) Genesis of the Marathon Cu-platinum group-element deposit, Port Coldwell Alkalic Complex, Ontario: A Midcontinent rift-related magmatic sulphide deposit. Economic Geology 89:131–149.

Heaman LM Machado N (1992) Timing and origin of midcontinent rift alkaline magmatism, North America: evidence from the Coldwell Complex. Contributions to Mineralogy and Petrology 110:289–303.

Heaman LM, Easton RM, Hart TR, Hollings P, MacDonald CA, Smyk M (2007) Further refinement to the timing of Mesoproterozoic magmatism, Lake Nipigon region, Ontario. Canadian Journal of Earth Sciences 44:1055–1086.

Hollings P, Smyk M, Heaman LM, Halls H (2010) The geochemistry, geochronology, and paleomagnetism of dikes and sills associated with the Mesoproterozoic Midcontinent Rift near Thunder Bay, Ontario, Canada. Precambrian Research 183: 553–571.

Joslin GD (2004) Stratiform palladium-platinum-gold mineralization in the Sonju Lake intrusion, Lake County, Minnesota. M.Sc. thesis, University of Minnesota.

Le Vaillant M, Barnes SJ, Mungall JE, Mungall EL (2017) Role of degassing of the Noril'sk nickel deposits in the Permian–Triassic mass extinction event. Proceedings of the National Academy of Sciences 114:2485–2490.

Miller JD (1998) Potential for reef-type PGE mineralization in the Duluth Complex: Evidence from the Layered Series at Duluth. The Minnesota Prospector, Special Issue, 8–12.

Miller JD Nicholson SW (2013) Geology and mineral deposits of the 1.1 Ga Midcontinent Rift in the Lake Superior region – An overview; in Field Guide to the Cu-Ni-PGE Deposits of the Lake Superior Region (ed) JD Miller. Precambrian Research Center Guidebook 13-1:1–50.

Mungall JE, Brenan JM, Godel B, Barnes SJ, Gaillard F (2015) Transport of metals and sulphur in magmas by flotation of sulphide melt on vapour bubbles. Nature Geoscience 8:216–219.

O'Brien S (2018) Geology of the Crystal Lake Gabbro and the Mount Mollie Dyke, Midcontinent Rift, Northwest Ontario. M.Sc. thesis, Lakehead University.

Ripley EM (2014) Ni-Cu-PGE mineralization in the Partridge River, South Kawishiwi, and Eagle intrusions: A review of contrasting styles of sulphide-rich occurrences in the Midcontinent rift system. Economic Geology 109:309–324.

Smith AR Sutcliffe RH (1987) Keweenawan intrusive rocks of the Thunder Bay area. Ontario Geological Survey, Miscellaneous Paper 137:248–255.

Song X, Wang Y, Chen L (2011) Magmatic Ni-Cu- (PGE) deposits in magma plumbing systems: Features, formation and exploration. Geoscience Frontiers 2:375–384.

Thomas B (2015) Geochemistry, sulfur isotopes and petrography of the Cu-Ni-PGE mineralized Crystal Lake intrusion, Thunder Bay, Ontario. M.Sc. thesis, Indiana University.